Small-scale parallel protein synthesis ● TIMING 1 h + an overnight reaction + 3 h

40| Keep the mRNA tubes in room temperature. Thaw the extract in water and put it on ice immediately after it has thawed. Thaw the creatine kinase solution on ice. Thaw 1× BSS on ice and mix it well. Spin down the thawed solutions.

41| Dispense 10 μl of 240 OD per ml extract and 0.8 μl of 1 mg ml^{-1} creatine kinase into each well of a microtiter plate on ice. This microtiter plate can be replaced with standard microtubes or PCR tubes if the number of the samples is small.

42| Resuspend the mRNA solutions, which contain white insoluble material, and transfer 10 μl of each suspension into each well of the microtiter plate. Mix the samples gently by pipetting, avoiding bubbles.

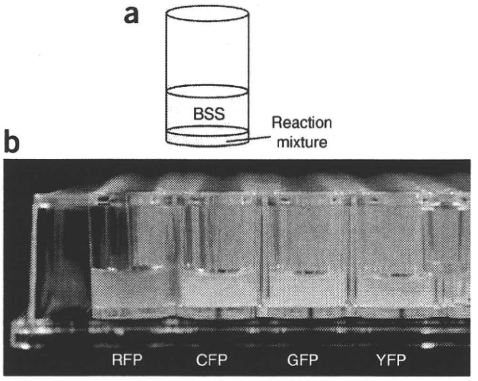

Figure 5 | A schematic representation of the bilayer to be formed at the start of the translation reaction (**a**) and a typical result of translation (**b**). (**a**) In the small-scale protein synthesis, the reaction mixture is layered under the buffered substrate solution (BSS). The two solutions will mix together gradually during incubation. (**b**) Fluorescent proteins synthesized in microtiter plate wells.

43| Dispense 206 μl of 1× BSS in each well of a flat-bottomed microtiter plate.

44| Take each of the mRNA/extract mixtures into a micropipette tip so that no air is at the end of the tip. Insert the tip at the bottom of a microtiter well containing 1× BSS carefully with holding the mixture within the tip and then carefully pump out the mixture under the buffer without mixing, avoiding bubbles, so that the mRNA/extract mixture and the buffer form a bilayer (**Fig. 5a**). Do not mix the samples.
▲ **CRITICAL STEP** Do not mix the samples. It is very important at the start of the reaction that the starting reaction mixture forms a distinct layer that forms a clear boundary with the upper BSS liquid.

45| Seal the wells to avoid evaporation. Be careful not to shake the plate too much.

46| Leave the plate in the air incubator at 15 °C for 20 h.

47| Analyze the sample (3–5 μl) on a standard SDS gel.
? TROUBLESHOOTING

Transcription of a pEU plasmid harboring a target ORF sequence ● TIMING 5–7 h excepting Step 48

48| Subclone the target ORF into pEU (**Fig. 2c**) and prepare the plasmid using a standard plasmid preparation kit, such as QIAGEN Plasmid Midi Kit. Dissolve the plasmid in the standard TE buffer. Determine the concentration and purity of the DNA sample by measuring the absorbance values at 260 and 280 nm. If the A_{260}/A_{280} ratio is not between 1.70 and 1.85, then further purify the sample by phenol/chloroform extraction, followed by chloroform extraction and ethanol precipitation with rinsing the pellet with 70% ethanol. Adjust the concentration to 1 μg μl^{-1} with TE.
▲ **CRITICAL STEP** It is recommended to always perform the appended purification steps, because most plasmid preparation kits use an RNase, and because even a small amount of RNase would inhibit the transcription and translation.
■ **PAUSE POINT** Plasmids can be stored for years at −20 °C.

49| Mix 25 μg of plasmid DNA in 250 μl of the transcription buffer containing 50 μl of 5× TB, 25 μl of 25 mM NTP, 250 U of RNase inhibitor and 250 U of SP6 RNA polymerase and incubate this mixture at 37 °C for 6 h. White insoluble material will be generated during transcription. Perform the control reaction with pEU-E01-DHFR or pEU-E01-GFP.

50| Check the sample in an agarose gel. Transcription stops partially at the plasmid replication origin.
■ **PAUSE POINT** The transcription product can be stored at −80 °C for several weeks. Transportation with dry ice is not recommended.
? TROUBLESHOOTING

Large-scale protein synthesis ● TIMING 1 h + an overnight reaction + 3 h

51| Put the mRNA tubes in room temperature. Thaw the extract in water and put it on ice immediately after it has thawed. Thaw the creatine kinase 20 mg ml^{-1} solution on ice. Thaw 1× BSS on ice and mix it well. Spin down the thawed solutions.

52| Dispense 250 µl of 240 OD per ml extract and 1 µl of 20 mg ml^{-1} creatine kinase into each fresh microtubes on ice.

53| Resuspend the mRNA solutions, which contain white insoluble material, and transfer 250 µl of each suspension into each microtube containing the extract and creatine kinase. Mix the samples gently by pipetting, avoiding bubbles.

54| Dispense 5.5 ml of 1× BSS in each well of a flat-bottomed six-well plate.

55| Take each of the mRNA/extract mixtures into a micropipette tip so that no air is at the end of the tip. Insert the tip at the bottom of a microtiter well containing 1× BSS carefully by holding the mixture within the tip and then carefully pump out the mixture under the buffer without mixing, avoiding bubbles, so that the mRNA/extract mixture and the buffer form a bilayer. Do not mix the samples. Do not shake the plate.
▲ **CRITICAL STEP** Do not mix the samples. It is very important at the start of the reaction that the starting reaction mixture forms a distinct layer that forms a clear boundary with the upper BSS liquid.

56| Seal the plate to avoid evaporation. Be careful not to shake the plate too much.

57| Leave the plate in the air incubator at 15 °C for 20 h.

58| After the incubation, mix the samples for further analyses.

59| To check the products, load 3 µl of the samples on a standard SDS gel.
? TROUBLESHOOTING

● TIMING
Steps 1–8, preparation of unwashed embryo particles: 2–3 d per 5 g embryo particles from 5 to 6 kg seeds
Steps 9–27, preparation of the extract: 1 d
Steps 28–37, template DNA preparation for small-scale parallel protein synthesis: 1 day
Steps 38 and 39, mRNA preparation for small-scale parallel protein synthesis: 5–7 h
Steps 40–47, small-scale parallel protein synthesis: 1 h + an overnight reaction (20 h) + 3 h
Step 48–50, transcription of a pEU plasmid harboring a target ORF sequence: 5–7 h excepting Step 48
Steps 51–59, large-scale protein synthesis: 1 h + an overnight reaction (20 h) + 3 h

? TROUBLESHOOTING
Troubleshooting advice can be found in **Table 2.** In our experience, most of the troubles come from a problem during the construction of the DNA molecules that are used for PCR and/or transcription.

TABLE 2 | Troubleshooting table.

Step	Problem	Possible reason	Solution
23	Low absorbance	Grinding was not sufficient	This could be foreseen by the color of the supernatant in Step 19
26	Absorbance lower than 240	Insufficient condensation in Step 24	Concentrate the sample again, or leave it as it is
29	No band	Bad template	Check the template cDNA. The plasmid should have the pUC origin and the cDNA sequence
		The specific primer does not hybridize well	Lower the annealing temperature of the PCR program. Extend the target region of the primer
		Primer-dimer involving the specific primer	Extend the target region of the primer
	Nonspecific bands	Hybridization of AODA2306 within the ORF	Try proceeding to Steps 30–37. If the result is still bad, try another primer that hybridizes near the replication origin. For screening purposes, judge if one wishes to stick to this sample
37	No band	Loss of the pellet in the Step 33 or 35	Restart from Step 30
	Nonspecific bands	Nonspecific hybridization within the ORF	Try translation if the main band is correct. For screening purposes, judge if one wishes to stick to this sample

(continued)

TABLE 2 | Troubleshooting table (continued).

Step	Problem	Possible reason	Solution
39	No band	dNTP instead of NTP added to the reaction	Try again being careful not to confuse NTP with dNTP
	Ladder in the high mobility region	Contamination by Rnases	Extract the template DNA with phenol/chloroform
	Unexpected low mobility extra bands	Efficient transcription	This usually causes no problem in translation
	Very bright bands	Sample is not denatured and is complexed with Spermidine	Denature the sample in a formamide loading dye, which may be the one used for denaturing gels, before applying to the gel
47 or 59	No product	Bad mRNA	Check the mRNA and template DNA again
	No or very faint band	Inefficient translation	Try the small-scale translation again with ^{14}C-labeled leucine added to the reaction and BSS and detect the product by autoradiography or by counting the radioactivity in the acid-insoluble fraction of the reaction mixture
		Alternative translation initiation (out of frame)	Eliminate Gs from between the E01 enhancer sequence and the initiation codon
	Doublet band	Alternative translation initiation (in frame)	Eliminate Gs from between the E01 enhancer sequence and the initiation codon
50	Smear or ladder in the high-mobility region	Contamination by RNase	Further purify the plasmid template as in Step 47
	No band	dNTP instead of NTP added to the reaction	Try again being careful not to confuse NTP with dNTP
		Bad plasmid	Check the plasmid DNA
59	No band	Bad plasmid	Check the plasmid DNA
	Unexpected bands in the low-mobility region	Post-translational modification	Post-translational modification may occur for some proteins We have no unified methodology

ANTICIPATED RESULTS

We show here a typical result of small-scale bilayer mode synthesis of fluorescent proteins (**Fig. 5b**). An SDS gel showing a typical result of synthesis of dihydrofolate reductase (DHFR) is in **Figure 6**. It is difficult to show an averaged amount of produced protein per 1-ml reaction because we do not have a reliable statistic data with the protocol shown here and because the productivity per reaction volume including BSS can vary with the relative volume of BSS to the reaction mixture. However, the average yield per

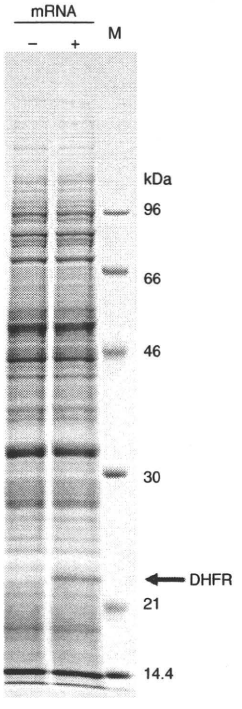

Figure 6 | A typical result of the small-scale bilayer synthesis of DHFR. DHFR was synthesized by the bilayer method using the CFS extract (CFS-TRI-1240), and a 3-μl aliquot of the mixed sample was separated on an SDS gel stained with CBB (Step 47). The left lane (mRNA+), a control reaction product with no mRNA added; the center lane (mRNA–), the product with the DHFR mRNA; and the right lane (M), marker proteins with molecular masses indicated on the right. The amount of DHFR synthesized was 80 ng μl^{-1} (1.8 mg per 1-ml extract). In the parallel protein synthesis experiments, the 'mRNA–' reaction can usually be omitted because different samples can serve as the markers indicating the positions of the bands of the wheat embryo proteins. Modified from a figure kindly provided by R. Morishita, CellFree Sciences.

1-ml extract may be around 0.3 mg both in the small- and large-scale bilayer method. In fact, the average amount per a 150-µl reaction containing 12 µl of the extract for the 13,000 different human ORFs was 4.2 µg, which means 0.35 mg per 1-ml extract[7].

ACKNOWLEDGMENTS This work was supported in part by the Special Coordination Funds for Promoting Science and Technology (Y.E.) and in part by a Grant-in-Aid for Scientific Research on the Priority Areas (No. 20034040 to K.T.) by the Ministry of Education, Culture, Sports, Science and Technology, Japan. We are grateful to Dr. R. Morishita and Mr. Y. Tanaka of CFS for providing pictures and for checking the paper.

AUTHOR CONTRIBUTIONS K.T. collected information and wrote the paper; T.S. prepared the data and pictures; and Y.E. supervised the study.

Published online at http://www.natureprotocols.com/.
Reprints and permissions information is available online at http://npg.nature.com/reprintsandpermissions/.

1. Spirin, A.S., Baranov, V.I., Ryabova, L.A., Ovodov, S.Y. & Alakhov, Y.B. A continuous cell-free translation system capable of producing polypeptides in high yield. *Science* **242**, 1162–1164 (1988).
2. Madin, K., Sawasaki, T., Ogasawara, T. & Endo, Y. A highly efficient and robust cell-free protein synthesis system prepared from wheat embryos: plants apparently contain a suicide system directed at ribosomes. *Proc. Natl. Acad. Sci. USA* **97**, 559–564 (2000).
3. Sawasaki, T., Ogasawara, T., Morishita, R. & Endo, Y. A cell-free protein synthesis system for high-throughput proteomics. *Proc. Natl. Acad. Sci. USA* **99**, 14652–14657 (2002).
4. Sawasaki, T. *et al.* A bilayer cell-free protein synthesis system for high-throughput screening of gene products. *FEBS Lett.* **514**, 102–105 (2002).
5. Endo, Y. & Sawasaki, T. Cell-free expression systems for eukaryotic protein production. *Curr. Opin. Biotechnol.* **17**, 373–380 (2006).
6. Takai, K., Sawasaki, T. & Endo, Y. Development of key technologies for high-throughput cell-free protein production with the extract from wheat embryos. *Adv. Protein Chem. Struct. Biol.* **75**, 53–84 (2008).
7. Goshima, N. *et al.* Human protein factory for converting the transcriptome into an *in vitro*-expressed proteome. *Nat. Methods* **5**, 1011–1017 (2008).
8. Tsuboi, T. *et al.* Wheat germ cell-free system-based production of malaria proteins for discovery of novel vaccine candidates. *Infect. Immun.* **76**, 1702–1708 (2008).
9. Sawasaki, T. *et al.* The wheat germ cell-free expression system: methods for high-throughput materialization of genetic information. *Methods Mol. Biol.* **310**, 131–144 (2005).
10. Sawasaki, T. & Endo, Y. Chapter 6. Protein expression in the wheat-germ cell-free system. In *Expression Systems* (eds. Dyson, M.R. & Durocher, Y.) 87–108 (Scion Publishing Ltd., Oxfordshire, Oxford, UK, 2007).
11. Endo, Y., Dohi, N. & Nakagawa, M. Germ extract for cell-free protein synthesis and process for producing the same. International Patent WO/2003/064671 filed 31 January 2003.
12. Kamura, N., Sawasaki, T., Kasahara, Y., Takai, K. & Endo, Y. Selection of 5′-untranslated sequences that enhance initiation of translation in a cell-free protein synthesis system from wheat embryos. *Bioorg. Med. Chem. Lett.* **15**, 5402–5406 (2005).
13. Masaoka, T., Nishi, M., Ryo, A., Endo, Y. & Sawasaki, T. The wheat germ cell-free based screening of protein substrates of calcium/calmodulin-dependent protein kinase II delta. *FEBS Lett.* **582**, 1795–1801 (2008).
14. Makino, S., Sawasaki, T., Tozawa, Y., Endo, Y. & Takai, K. Covalent circularization of exogenous RNA during incubation with a wheat embryo cell extract. *Biochem. Biophys. Res. Commun.* **347**, 1080–1087 (2006).
15. Hirano, N., Sawasaki, T., Tozawa, Y., Endo, Y. & Takai, K. Tolerance for random recombination of domains in prokaryotic and eukaryotic translation systems: limited interdomain misfolding in a eukaryotic translation system. *Proteins* **64**, 343–354 (2006).
16. Nureki, O. *et al.* Deep knot structure for construction of active site and cofactor binding site of tRNA modification enzyme. *Structure* **12**, 593–602 (2004).
17. Ikeda, K. *et al.* Immobilization of diverse foreign proteins in viral polyhedra and potential application for protein microarrays. *Proteomics* **6**, 54–66 (2006).
18. Matsumoto, K. *et al.* Production of yeast tRNA (m^7G46) methyltransferase (Trm8-Trm82 complex) in a wheat germ cell-free translation system. *J. Biotechnol.* **133**, 453–460 (2008).
19. Kanno, T., Kasai, K., Ikejiri-Kanno, Y., Wakasa, K. & Tozawa, Y. *In vitro* reconstitution of rice anthranilate synthase: distinct functional properties of the alpha subunits OASA1 and OASA2. *Plant Mol. Biol.* **54**, 11–22 (2004).
20. Takahashi, H., Nozawa, A., Seki, M., Shinozaki, K., Endo, Y. & Sawasaki, T. A simple and high-sensitivity method for analysis of ubiquitination and polyubiquitination based on wheat cell-free protein synthesis. *BMC Plant Biol.* **9**, 39 (2009).
21. Kanno, T. *et al.* Sequence specificity and efficiency of protein N-terminal methionine elimination in wheat-embryo cell-free system. *Protein Expr. Purif.* **52**, 59–65 (2007).
22. Kobayashi, T., Kodani, Y., Nozawa, A., Endo, Y. & Sawasaki, T. DNA-binding profiling of human hormone nuclear receptors via fluorescence correlation spectroscopy in a cell-free system. *FEBS Lett.* **582**, 2737–2744 (2008).
23. Sawasaki, T. *et al.* Arabidopsis HY5 protein functions as a DNA-binding tag for purification and functional immobilization of proteins on agarose/DNA microplate. *FEBS Lett.* **582**, 221–228 (2008).
24. Kanno, T. *et al.* Structure-based *in vitro* engineering of the anthranilate synthase, a metabolic key enzyme in the plant tryptophan pathway. *Plant Physiol.* **138**, 2260–2268 (2005).
25. Morita, E.H., Sawasaki, T., Tanaka, R., Endo, Y. & Kohno, T. A wheat germ cell-free system is a novel way to screen protein folding and function. *Protein Sci.* **12**, 1216–1221 (2003).
26. Vinarov, D.A. *et al.* Cell-free protein production and labeling protocol for NMR-based structural proteomics. *Nat. Methods* **1**, 149–153 (2004).
27. Vinarov, D.A., Loushin Newman, C.L. & Markley, J.L. Wheat germ cell-free platform for eukaryotic protein production. *FEBS J.* **273**, 4160–4169 (2006).
28. Morita, E.H. *et al.* A novel way of amino acid-specific assignment in ^{1}H-^{15}N HSQC spectra with a wheat germ cell-free protein synthesis system. *J. Biomol. NMR* **30**, 37–45 (2004).
29. Kohno, T. Production of proteins for NMR studies using the wheat germ cell-free system. *Methods Mol. Biol.* **310**, 169–185 (2005).
30. Kohno, T. & Endo, Y. Production of protein for nuclear magnetic resonance study using the wheat germ cell-free system. *Methods Mol. Biol.* **375**, 257–272 (2007).
31. Kainosho, M. *et al.* Optimal isotope labelling for NMR protein structure determinations. *Nature* **440**, 52–57 (2006).
32. Miyazono, K. *et al.* Novel protein fold discovered in the PabI family of restriction enzymes. *Nucleic Acids Res.* **35**, 1908–1918 (2007).
33. Abe, M. *et al.* Detection of structural changes in a cofactor binding protein by using a wheat germ cell-free protein synthesis system coupled with unnatural amino acid probing. *Proteins* **67**, 643–652 (2007).
34. Kawasaki, T., Gouda, M.D., Sawasaki, T., Takai, K. & Endo, Y. Efficient synthesis of a disulfide-containing protein through a batch cell-free system from wheat germ. *Eur. J. Biochem.* **270**, 4780–4786 (2003).
35. Nozawa, A. *et al.* A cell-free translation and proteoliposome reconstitution system for functional analysis of plant solute transporters. *Plant Cell Physiol.* **48**, 1815–1820 (2007).
36. Goren, M.A. & Fox, B.G. Wheat germ cell-free translation, purification, and assembly of a functional human stearoyl-CoA desaturase complex. *Protein Expr. Purif.* **62**, 171–178 (2008).
37. Kaiser, L., Graveland-Bikker, J., Steuerwald, D., Vanberghem, M., Herlihy, K. & Zhang, S. Efficient cell-free production of olfactory receptors: detergent optimization, structure, and ligand binding analyses. *Proc. Natl. Acad. Sci. USA* **105**, 15726–15731 (2008).

technical notes Journal of proteome research

Simple Screening Method for Autoantigen Proteins Using the N-Terminal Biotinylated Protein Library Produced by Wheat Cell-Free Synthesis

Kazuhiro Matsuoka,[†] Hiroaki Komori,[‡,§] Masato Nose,[‡,∥] Yaeta Endo,[*,†,∥,⊥,#] and Tatsuya Sawasaki[*,†,∥,⊥,#]

Cell-Free Science and Technology Research Center, Ehime University, 3 Bunkyo-cho, Matsuyama, Ehime 790-8577, Japan, Department of Pathogenomics, Ehime University Graduate School of Medicine, Toon, Ehime 791-0295, Japan, Proteo-Medicine Research Center, Ehime University, Toon, Ehime 791-0295, Japan, The Venture Business Laboratory, Ehime University, 3 Bunkyo-cho, Matsuyama, Ehime 790-8577, Japan, and RIKEN Systems and Structural Biology Center, 1-7-22 Suehiro-cho, Tsurumi-ku, Yokohama, Kanagawa 230-0045, Japan

Received November 18, 2009

Abstract: Autoimmune diseases are a heterogeneous group of diseases characterized by immune reactions against either a major or a limited number of the bodies own autoantigens, causing inflammation and damage to tissues and organs. Thus, identification of autoantigens is an important first step to understanding autoimmune diseases. Here we demonstrate a simple screening method for identification of autoantigens reacting with patient serum antibodies by combination of an N-terminal biotinylated protein library (BPL), produced using a wheat cell-free protein production system, and a commercially available luminescence system. Optimization studies using well-characterized autoantigens showed specific interactions between N-terminal biotinylated proteins and antibody that were sensitively detected under homogeneous reaction conditions. In this optimized assay, 1 μL of the translation mixture expressing the biotinylated proteins produced significant luminescence signal by addition of diluted serum between 1:500 and 1:10 000 in 25 μL of reaction volume. For the BPL construction, 214 mouse genes, consisting of 103 well-known autoantigens and 111 genes in the mouse autoimmune susceptibility loci, and the sera of MRL/lpr mouse were used as an autoimmune model. By this screening method, 25 well-known autoantigens and 71 proteins in the loci were identified as autoantigen proteins specifically reacting with sera antibodies. Cross-referencing with the Gene Ontology Database, 26 and 38 of autoantigen proteins were predicted to have nuclear localization and identified as membrane and/or extracellular proteins. The immune reaction of six randomly selected proteins was confirmed by immunoprecipitation and/or immunoblot analyses. Interestingly, three autoantigen proteins were recognized by immunoprecipitation but not by immunoblot analysis. These results suggest that the BPL-based method could provide a simple system for screening of autoantigen proteins and would help with identification of autoantigen proteins reacting with antibodies that recognize folded proteins, rather than denatured or unfolded forms.

Keywords: autoantigen • autoimmunity • biomarker • cell-free protein production • Gene Ontology • high-throughput screening • MRL/lpr mouse • proteomics

Introduction

Autoimmune diseases are generally characterized by the body's immune responses being directed against its own tissues, causing prolonged inflammation and subsequent tissue destruction.[1] A hallmark of autoimmune diseases is the production of autoantibodies such as antinuclear, anti-Sm and anti-dsDNA in systemic lupus erythematosus (SLE),[2] and the presence of RF, hnRNP A2 and calpastatin in rheumatoid arthritis (RA).[3] However, there are still a lot of autoimmune diseases for which antibodies have not been identified.[2] To understand the molecular mechanisms in autoimmune diseases, it is important to identify the relevant autoantigens, and moreover, they could be pathogenic in these diseases. It is widely hypothesized that proteins are the major antigenic targets associated with autoimmune diseases.[2] Therefore, development of methods that allow large-scale screening of autoantigen proteins is indispensable for elucidation and diagnosis of the autoimmune diseases.

To date, autoantigen proteins have been detected as antigenic molecules that are recognized by humoral antibodies, including those in serum.[2] The large-scale screening of au-

* To whom correspondence should be addressed. Yaeta Endo, Cell-Free Science and Technology Research Center, Ehime University, Bunkyo-cho, 3-ban, Matsuyama 790-8577, Japan. Tel. +81-89-927-9936. Fax +81-89-927-9941. E-mail yendo@eng.ehime-u.ac.jp. Tatsuya Sawasaki, Cell-Free Science and Technology Research Center, Ehime University, Bunkyo-cho, 3-ban, Matsuyama 790-8577, Japan. Tel. +81-89-927-8530. Fax +81-89-927-9941. E-mail sawasaki@eng.ehime-u.ac.jp.

† Cell-Free Science and Technology Research Center, Ehime University.

‡ Ehime University Graduate School of Medicine.

§ Deceased March 7, 2009.

∥ Proteo-Medicine Research Center, Ehime University.

⊥ The Venture Business Laboratory, Ehime University.

RIKEN Systems and Structural Biology Center.

Published on Web 06/24/2010

10.1021/pr9010553

toantigen proteins reacting with patient serum antibodies has been carried out by mainly three technologies: serological proteome analysis (SERPA), serological expression cloning (SEREX) and protein microarray.[4] The utility of SERPA and SEREX for this screening is limited because particular cells and tissues are generally used as antigen resources in these systems and they are dependent on artificial membranes for immunoblotting which do not maintain native protein structure.[5] Recent advances in protein microarray technology have allowed large-scale screening of autoantigens reacting with the sera of patients suffering from autoimmune disorders and cancer.[5−7] However, protein microarray is not yet a commonly used biochemical tool for screening.[8] One issue with protein microarrays is that purified recombinant proteins are required, which demonstrate batch-to-batch variation and limited stability and shelf life.[5] Additionally, it is difficult to maintain the functional form of a protein after their immobilization on a microplate. Many proteins needed to be appropriately oriented for proper functioning.[9] In fact, a number of spotted autoantigens were not always detectable with planar arrays, presumably due to loss of three-dimensional structures, steric interference or electrostatic repulsion.[6]

In this work, we developed a novel autoantigen protein screening method that overcame the following issues highlighted above: (1) utilization of a high-throughput and genome-wide protein expression system, (2) specific protein labeling for assay using unpurified protein samples and (3) high-throughput detection system of properly folded antigen. Toward the first, we recently developed an automated protein production robot utilizing a high-throughput wheat embryo derived cell-free protein production system.[10,11] The combination of an automatic cell-free protein production system and the full-length cDNA allowed for facile construction of a robust protein library.[12] To enhance the utility of the library, per the second issue above, specific labeling of each protein is required for efficient detection. We selected biotin as the labeling compound because it is readily available and demonstrates high specificity for streptavidin binding. The biotinylated protein library (BPL) was constructed using target proteins fused to a biotin ligation site (bls), and expression was performed in the presence of biotin and biotin ligase (BirA).[13] BirA from *Escherichia coli* specifically conjugates a single biotin on the bls. This method was compatible with our high-throughput automated platform. To address the third issue, we selected the luminescent high-throughput protein−protein interaction detection system AlphaScreen.[14,15] This method can directly recognize biotinylated protein in the translation mixture without purification and the use of any potential protein denaturants allowing for antibody detection of natively folded antigens.[15] In this work, we demonstrate a simple BPL-based method for screening of autoantigen proteins reacting with the sera of an autoimmune disease model mouse, MRL/Mp-*lpr*/*lpr* (MRL/lpr), and the detection of the autoantigen proteins by immunoprecipitation, rather than immunoblotting methods often accompanied by protein denaturation.

Materials and Methods

General. The following procedures have been either described in detail or cited previously:[10,16] generation of DNA template by polymerase chain reaction (PCR) using "split-primer"; synthesis of mRNA and protein in parallel; estimation of the amounts of synthesized proteins by densitometric scanning of the Coomassie brilliant blue (CBB)-stained bands or by autoradiography. The wheat germ extract was purchased from Cell-Free Science Co. (Yokohama, Japan). Anti-p53 monoclonal antibody (D01) was purchased from Santa Cruz Biotechnology (Santa Cruz, CA). Mouse serum for mouse immunoglobulin in Figure 1 was purchased from Calbiochem (Darmstadt, Germany). Other reagents used in this study were described previously.[10,15]

Serum Samples. MRL/lpr mice were originally purchased from the Jackson Laboratory (Bar Harbor, ME). All of the mice used in this paper were maintained in clean rooms at the Animal Research Institute, School of Medicine, Ehime University. Sera of female mice were collected from 15 mice and pooled and stocked in −20 °C until use. All experiments were done according to the Guidelines for the Care and Use of Laboratory Animals at Ehime University.

DNA Template Construction for the BPL. Functional annotation of mouse (FANTOM) as a mouse full-length cDNA resource is purchased from a company (Danaform, Tokyo, Japan). The DNA templates for transcription were constructed by "split-primer" PCR technique described previous reports.[10,17] The first PCR was amplified with 10 nM of each of the following primers: a gene specific primer, 5′- CCACCCACCACCACCAAT-Gnnnnnnnnnnnnnnnnnn (n denotes the coding region of the target gene), and AODA2303 (5′-GTCAGACCCCGTAGAAAAGA) or AODS (5′-TTTCTACGGGGTCTGACGCT). The second PCR products for protein synthesis were constructed with 100 nM SPu 5′-GCGTAGCATTTAGGTGACACT, 1 nM deSP6E02bls-S1 (5′-GGTGACACTATAGAACTCACCTATCTCTCTACACAAAACA-TTTCCCTACATACAACTTTCAACTTCCTATTATGGGCCTGAAC-GACATCTTCGAGGCCCAGAAGATCGAGTGGCACGAACTCCA-CCCACCACCACCAATG) and 100 nM AODA2303 or AODS. By this "split-primer" PCR, the bls was fused onto the N-terminals of all the genes for protein biotinylation.[13]

Construction of the BPL by the Cell-Free Protein Synthesis System. Cell-free construction of the BPL is based on the previously described bilayer diffusion system in which 1 μL (50 ng) crude cell-free expressed BirA was added to the translation layer and 500 nM D-biotin (Nacalai Tesque, Kyoto, Japan) was added to both the translation and substrate layers.[13,18] *In vitro* transcription and cell-free protein synthesis for the BPL were carried out using the GenDecoder1000 robotic synthesizer (CellFree Sciences Co.) as previously described.[17,19]

Detection of Biotinylated Protein−Antibody Reaction by Luminescence Method. The AlphaScreen assay was performed according to the manufacture's protocol (PerkinElmer Life and Analytical Sciences, Boston, MA). Reactions were carried out in 25 μL of reaction volume in 384-well Optiwell microtiter plates (PerkinElmer Life and Analytical Sciences). For the antigen−autoantibody reaction, the translation mixture expressing the biotinylated protein was mixed with MRL/lpr mouse serum diluted 1:600 in 15 μL of reaction buffer [100 mM Tris-HCl (pH 8.0), 0.01% (v/v) Tween-20 and 0.1% (w/v) bovine serum albumin] and incubated at 26 °C for 30 min. Subsequently, 10 μL of streptavidin-coated donor beads and protein A-conjugated acceptor beads (PerkinElmer Life and Analytical Sciences) were added to a final concentration of 20 μg/mL per well and incubated at 26 °C for 1 h in a dark box. Fluorescence emission was measured with the EnVision plate reader (PerkinElmer Life and Analytical Sciences), and the resultant data were analyzed using the AlphaScreen detection program. All repetitive mechanical procedures were performed by a Biomek FX robotic workstation (Beckman Coulter, Fullerton, CA).

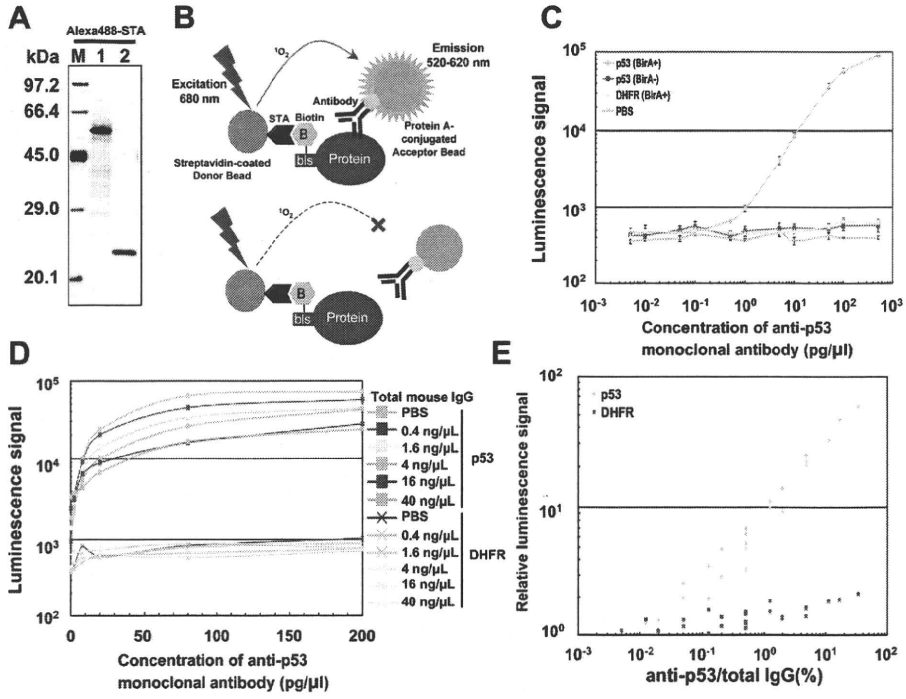

Figure 1. Sensitivity and specificity for detection of biotinylated p53 protein–antibody complex. (A) Biotinylated p53 (lane 1) and dihydrofolate reductase (DHFR) (lane 2) was detected by immunoblotting analysis using Alexa488-STA. M indicates protein molecular weight marker. (B) Schematic diagram of detection of biotinylated protein–antibody interaction by luminescence analysis. When a biotinylated protein and antibody interact (upper panel), Protein A-conjugated acceptor beads bound to antibody and streptavidin (STA)-coated donor beads bound to biotinylated protein are in close proximity. Upon excitation at 680 nm, a singlet oxygen is generated by the donor beads, transferred to the acceptor beads within 200 nm, and the resultant reaction emits light at 520–620 nm. This emission is measured using an EnVision. (C) Detection sensitivity of the antibody concentration measured by luminescence analysis. Translation mixture (1 μL) expressing biotinylated or nonbiotinylated p53 protein and biotinylated DHFR were incubated with various concentration of monoclonal antibody from 5×10^{-3} to 5×10^{2} pg/μL. (D) Biotinylated protein–antibody complex by interaction between biotinylated p53 protein and the monoclonal antibody in the presence of mouse serum was detected by luminescence analysis. (E) Minimum IgG amount in the presence of mouse serum to detect biotinylated p53 proteins. The relative luminescence signals between the specific luminescence and background signals indicated in the *y*-axis.

Immunoblotting. Biotinylated proteins were partially purified using streptavidin-coated beads (Streptavidin Sepharose High Performance, GE Healthcare, Buckinghamshire, U.K.). Translation mixtures (150 μL) including biotinylated proteins were mixed with 10 μL of streptavidin-coated beads for 30 min. The resin was washed three times with PBS buffer and then boiled in 15 μL of SDS sample buffer (50 mM Tris-HCl pH 6.8, 2% SDS, 10% glycerol and 0.2% bromophenol blue). After separation by 12.5% SDS-PAGE, the proteins were transferred to PVDF membrane (Millipore, Bedford, MA) by semidry blotting. The membrane was soaked in PBS containing 5% (w/v) skim milk for 1 h and then incubated with serum diluted 1:200 in PBS containing 0.1% (v/v) Tween 20 (PBST) for 1 h. After washing three times in PBST, it was incubated in PBS including goat-antimouse IgG-HRP antibody (GE Healthcare) diluted 1:10 000 for 30 min. After washing three times in PBST, the blots were detected by the ECL plus detection system (GE Healthcare) by using Typhoon 9400 imaging system (GE Healthcare) according to the manufacturer's protocol.

Immunoprecipitation. Fifty microliters of translation mixture expressing biotinylated proteins were incubated in 50 μL of IP buffer [PBS containing 0.1% (w/v) BSA, 0.15% (v/v) Tween 20] with 1 μL of undiluted serum overnight at 4 °C. Immobilized Protein A sepharose (20 μL of 50% slurry, Protein A Sepharose 4 Fast Flow, GE Healthcare) in IP buffer was added to each sample and incubated for 60 min at 4 °C. After centrifugation for 1 min at 900× *g*, samples were washed three times with IP buffer and then boiled for 5 min in SDS sample buffer. After separation by 12.5% SDS-PAGE, the samples were transferred to a Hybond-LFP PVDF membrane (GE Healthcare). After blocking with 5% (w/v) skim milk in PBS overnight at 4 °C, the membranes were soaked in PBS buffer containing 10 μg/mL streptavidin Alexa Fluor 488 conjugate (Alexa488-STA) (Invitrogen, Carlsbad, CA) and were washed three times with PBST. The biotinylated proteins on membrane were detected by Typhoon 9400 imaging system (GE Healthcare) according to the manufacturer's protocol.

Results

Sensitivity and Specificity for Detection of Antigen–Antibody Interaction Using Biotinylated p53 Protein. We adapted that AlphaScreen technology toward detecting interactions between antigen protein and antibody. To validate this technique, we used p53 protein, a well-characterized antigen protein.[20] Biotinylated or nonbiotinylated recombinant p53 and biotinylated recombinant dihydrofolate reductase (DHFR), serving as negative control, were synthesized by the wheat cell-free system (Figure 1A). For the analysis of antigen protein–antibody interaction, the translation mixture was used without any purification. In the AlphaScreen system, interaction of the biotinylated protein and antibody in sera results in a biotinylated protein–antibody complex that is captured simultaneously by the streptavidin-coated donor beads and the protein

A-conjugated acceptor bead. The resultant proximity of the acceptor and donor bead generates the luminescent signal upon irradiation at 680 nm. This is illustrated in Figure 1B.

For biotinylation of the target protein, the N-terminus of the target was fused to the bls, and the cell-free system was supplemented with BirA and biotin.[13] This biotin ligation method yields a biotin labeling on the bls, indicating a specific recognition of the target protein by AlphaScreen. To investigate the specificity and sensitivity of the antibody detection, translation mixtures expressing biotinylated or nonbiotinylated p53 protein were incubated with various concentrations of monoclonal antibody, ranging from 5×10^{-3} to 5×10^{2} pg/μL. This luminescence method specifically detected interaction of monoclonal antibody and the biotinylated p53 from the unpurified translation mixture, whereas nonbiotinylated p53 and biotinylated DHFR did not produce a significant luminescent signal (Figure 1C). In this condition, the biotinylated p53 was detected by anti-p53 antibody at concentrations as low as 0.5 pg/μL. Next, we investigated whether this luminescence method could detect the biotinylated protein–antibody complex in the presence of mouse serum. Translation mixture expressing biotinylated p53 protein was incubated with various concentrations of monoclonal antibody from 2 to 200 pg/μL and mouse immunoglobulin from 0.4 to 40 ng/μL. Figure 1D showed that this method could specifically detect the immunocomplex of biotinylated p53 protein and monoclonal antibody in the presence of an excess of mouse immunoglobulin. In addition, comparison between the specific luminescence and background signals indicated that biotinylated p53 could be detected at more than 0.05% of anti-p53 antibody in mouse serum (Figure 1E). These results indicate that this system is a highly specific and sensitive method for detection of interaction between biotinylated recombinant protein and antibody in whole serum.

Detection of Autoantibodies against Hars and LmnB2 Proteins in sera of MRL/lpr Mice. We next tested our protocol for the well-characterized autoantigens histidyl-tRNA synthetase (Hars)[21] and lamin B2 (LmnB2)[22] in the autoimmune disease model mouse MRL/lpr.[23] To determine the assay conditions using serum samples, biotinylated recombinant Hars and LmnB2 proteins were used (Figure 2A) to detect autoantibody in the sera of MRL/lpr mice. Cell-free synthesis of biotinylated Hars and LmnB2 demonstrated yields of 820 and 600 nM, and 43.0 and 56.4% of biotinylation, indicating biotinylated Hars and LmnB2 proteins were 354.4 and 338.5 nM, respectively. Various volumes (0.003 to 4 μL) of translation mixture expressing biotinylated Hars or LmnB2 protein were incubated with the serum of MRL/lpr mouse (final 1:1000 dilution) in 25 μL of reaction volume (Figure 2B). Significant luminescent signals were observed at additions of biotinylated Hars or LmnB2 proteins between 0.01 and 1 μL, which corresponds to biotinylated protein concentrations between 0.14 and 14 nM or 0.13 and 13 nM, respectively. Also serum dilutions between 1:500 and 1:10 000 produced high luminescence signal in 25 μL of reaction volume using 1 μL of the translation mixtures (Figure 2C). These results mean that five micro litter of serum and 200 μL of cell-free translation mixture expressing biotinylated proteins would be sufficient for 200 assays. Taken together, these results suggest that the luminescence method using cell-free expressed biotinylated proteins would be useful for screening the reaction of autoantigen proteins with autoantibodies in serum.

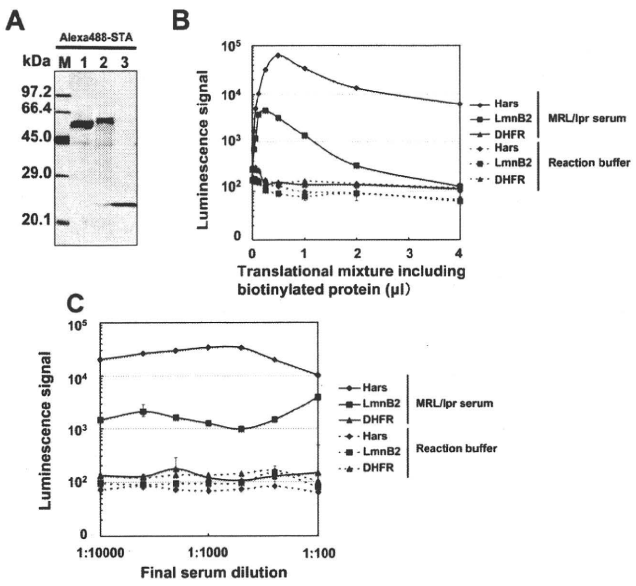

Figure 2. Detection of autoantibodies against Hars and LmnB2 proteins. (A) Biotinylated histidyl-tRNA synthetase (Hars) (lane 1), and lamin B2 (LmnB2) (lane 2) and DHFR (lane 3) proteins were detected by immunoblotting analysis using Alexa488-STA. M indicates protein molecular weight marker. (B) Various volumes (0.003 to 4 μL: representing 2.5–3280 nM Hars, 1.8–2400 nM LmnB2 and 6.4–8520 nM DHFR) of translation mixture expressing biotinylated Hars, LmnB2 or DHFR proteins were incubated with serum of MRL/lpr mouse sera (final 1:1000 dilution) in 25 μL of reaction volume. (C) Serum dilution between 1:100 and 1:10 000 was incubated with 1 μL of the translation mixtures in 25 μL of reaction volume.

Construction of the BPL by the Wheat Cell-Free Protein Production System. It has long been thought that comprehensive screening using a protein library is a strong tool for identification of antigen proteins.[12,24,25] The scheme for the BPL-based screening is shown in Figure 3A. To construct the N-terminal BPL, we selected 226 genes (Supplementary Table 1, Supporting Information) that included well-known autoantigen proteins and proteins coded by genes in the mouse autoimmune susceptibility loci[26] from the mouse full-length cDNA resource (FANTOM).[27,28] For biotinylation, a bls was fused onto 5′ site of a target gene by "split-primer" PCR.[13] Using the PCR, 222 (98.2%) out of 226 genes were successfully amplified and of those, 217 (96%) were transcribed. Synthesis of biotinylated proteins was performed on the GenDecoder1000,[19] and expression confirmed by SDS-PAGE combined with immunoblot analysis using Alexa488-STA (Figure 3B). Finally 214 clones (94.6%) were produced as biotinylated proteins (Supplementary Table 1, Supporting Information) at maximum and minimum concentrations of 500 and 10 nM respectively (data not shown). From our results in Figure 2B, the immunoresponse of biotinylated proteins could be detected below 0.2 nM by the luminescence method, indicating that all 214 proteins are at concentrations viable for screening. Therefore, we used these proteins as the BPL for screening of autoantigen proteins.

BPL-Based Screening of Autoantigen Proteins Using the MRL/lpr Mouse Sera. To identify autoantigen proteins reacting with antibodies in serum of autoimmune disease mice, the BPL and sera from pools of MRL/lpr or normal mouse sera (NMS)

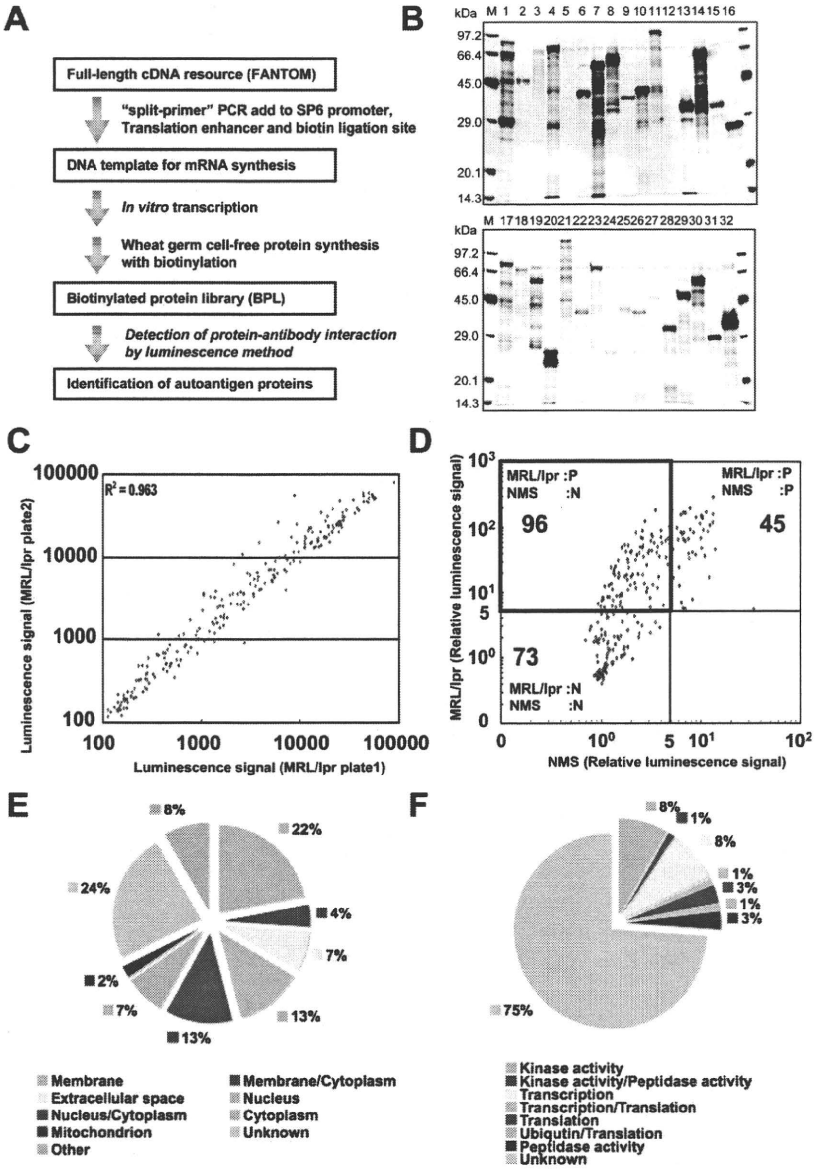

Figure 3. BPL-based screening of autoantigen proteins using the MRL/lpr mouse sera. (A) Schematic of the BPL-based screening method. (B) Thirty-two randomly selected biotinylated proteins of the BPL were detected by immunoblotting analysis using Alexa488-STA. (C) Scatter plot showing the luminescent signals in each well of two independent screening data sets using MRL/lpr mouse sera. The *x*-axis indicates luminescence signals in MRL/lpr plate 1 whereas the *y*-axis represents those in MRL/lpr plate 2. (D) Each data point represents luminescence signals using MRL/lpr mouse sera or normal mouse sera (NMS). The *x*-axis indicates luminescence signals in NMS whereas the *y*-axis represents those in MRL/lpr mice. (E, F) Ninety-six proteins identified as autoantigen proteins were grouped by protein localization in cells (E) Membrane (GO:0016020), Nucleus (GO:0005634), Cytoplasm (GO:0005737), Extracellular region (GO: 0005576) and Mitochondrion (GO:0005739) and biological function/process (F) Kinase activity (GO:0016301), Peptidase activity (GO: 0008233), Ubiquitin (GO:0005551), Translation (GO:0006412) and Transcription (GO:0006350) according to Gene Ontology Database. Minor groups less than 3 proteins were belonged to "Other" group. More detailed information on individual proteins was indicated in the Table 1.

were used. In each well of a 384-well plate, a translation mixture expressing biotinylated protein was incubated with either serum for 30 min, and subsequently a mixture of donor and acceptor beads was added to each well (see Figure 1B). After incubation, antigen−antibody reaction of the BPL was detected by the luminescence assay as described above. As shown in the scatter plot (Figure 3C), the intensity of paired luminescent signals in each well of two independent screening data sets (plate 1 and 2) using MRL/lpr mouse sera showed a linear distribution with a R^2 of 0.963, indicating reproducibly sufficient score for screening. We then compared the luminescent signals of the BPL reacted with MRL/lpr sera and NMS (Figure 3D). In this assay, only 141 of the 214 proteins in the BPL were identified as positive clones, which was indicated by a luminescence signal 5-fold higher than the average background signal. Only 96 proteins in the 141 positive clones reacted with MRL/lpr sera, whereas the remaining 45 proteins interacted with both sera. From these results, 96 proteins were identified as autoantigen proteins in MRL/lpr mice (Table 1, upper left panel in Figure 3D). In these MRL/lpr autoantigen proteins, 25 well-known autoantigens were included, and 71 out of 96 clones were coded in the genetic loci on chromosome 10; 40 cM, chromosome 15; 18 cM and chromosome 19; 49 cM,[26] indicating that this screening identified new MRL/lpr sera

Table 1. List of 96 Identified Proteins As Autoantigen Proteins

gene symbol	source[a]	M_w (kDa)	MRL/lpr[b]	NMS[b]	Gene Ontology[c]	
					cellular location	biological function/process
Agpat3	Chr 10_40	43.3	49.7	2.6	Me	
Bcr	Chr 10_40	35.3	6.4	1.5		K
Unc5b	Chr 10_40	103.7	42.3	3.6	Me	
Pyp	Chr 10_40	33.0	6.3	1.3		
Cdc2a	Chr 10_40	34.1	11.9	3.6	N	K
Cnnm2	Chr 19_49	96.6	64.4	4.4	Me	
Thop1	Chr 10_40	78.0	38.9	2.3	C	K, P
Hhex[d]	Chr 19_49	30.0	54.7	1.9	N	Tc
Palm	Chr 10_40	41.6	59.4	4.1	C, Me	
Gnaz	Chr 10_40	40.8	72.2	5.0	Me	
2610028F08Rik	Chr 15_18	28.3	17.9	1.7		
Ank	Chr 15_18	54.3	55.7	1.7	Me	
Nov	Chr 15_18	38.8	20.4	1.5	E	
Neurl	Chr 19_49	36.0	58.0	4.8		
Gpam	Chr 19_49	93.4	54.2	2.6	Mi, Me	
Ncald	Chr 15_18	22.2	5.9	1.1		
Wnt8b	Chr 19_49	40.5	13.8	2.7	E	
Timp3	Chr 10_40	24.2	19.8	2.3	Me, E	K
Osr2	Chr 15_18	30.6	17.2	1.5	N	
Nnp1	Chr 10_40	54.6	51.3	3.7		
Nfic	Chr 10_40	48.8	80.4	3.2	N	Tc
Pfkl	Chr 10_40	85.4	8.3	3.1	C	K
Slc18a2	Chr 19_49	55.8	72.5	2.5	C, Me	
Sgta[d]	Chr 10_40	34.2	23.0	1.3		
Hps6	Chr 19_49	87.3	59.5	3.4		
Sgpl1	Chr 10_40	63.7	90.9	4.0	Me	
Pdxk	Chr 10_40	35.1	8.1	1.0	C	K
Pwp2h	Chr 10_40	102.9	36.3	2.7		
Psap	Chr 10_40	61.1	42.2	2.4	Mi, E	
Fzd6	Chr 15_18	79.1	92.0	2.6	Me	
Ilvbl	Chr 10_40	68.2	45.8	3.0	Me	
Itgb2	Chr 10_40	84.9	41.7	2.9	Me	
Cstb	Chr 10_40	11.0	18.9	1.4	N, C	
Gstt2	Chr 10_40	27.6	25.1	1.3	N, C	
Bsg	Chr 10_40	29.7	20.4	1.3	Me	
Cpn1	Chr 19_49	52.1	6.1	1.0	E	P
Eif3s6	Chr 15_18	52.0	8.7	1.2		
Timm9	Chr 10_40	10.4	14.2	2.2	Mi, Me	
Ndufs7	Chr 10_40	24.7	11.8	2.9	Mi, Me	
Psd	Chr 19_49	12.4	51.6	2.4	Me	
Tfam	Chr 10_40	28.0	17.8	2.0	N, Mi	Tc
Ppap2c	Chr 10_40	31.2	51.2	1.6	Me	
Gpx4	Chr 10_40	22.1	18.1	1.5	N, C, Mi, Me	
Pcbd1	Chr 10_40	12.0	44.4	2.0	N, C	Tc
Ins1	Chr 19_49	12.2	30.1	1.9	E	
Mrpl54	Chr 10_40	15.4	8.5	1.0	Mi	
Oaz1	Chr 10_40	25.1	11.4	1.3		
Cxxc6	Chr 10_40	25.6	32.1	1.5		
Sdc2	Chr 15_18	22.1	42.5	2.0	Me	
Npm3	Chr 19_49	19.0	13.1	1.2	N	Tc
Eif4ebp2	Chr 10_40	12.9	7.6	1.0	Tl	
Ddt	Chr 10_40	13.1	5.1	0.9	C	
Pah	Chr 10_40	51.8	32.1	2.2		
Peo1	Chr 19_49	77.0	6.8	0.9	Mi	
Cabin1	Chr 10_40	65.2	13.8	1.3	N	
Lilrb4	Chr 10_40	37.5	9.0	1.4	Me	
Casp7	Chr 19_49	34.1	7.6	1.3	C	P
Matk	Chr 10_40	53.6	72.9	4.0	C, Me	K
Egr2	Chr 10_40	49.8	74.7	3.2	N	Tc
Slc1a6[d]	Chr 10_40	60.8	126.0	2.7	Me	
Adn	Chr 10_40	28.1	63.8	3.1		
Gna11	Chr 10_40	42.0	69.7	4.7		
Tbxa2r	Chr 10_40	37.1	43.9	1.8	Me	
Trhr	Chr 15_18	44.6	188.7	3.5	Me	
Ube2g2	Chr 10_40	33.0	16.0	1.8		U, Tl
Madcam1	Chr 10_40	43.6	33.5	1.8	Me	
Pcdh15	Chr 10_40	129.9	70.6	2.6	C, Me	
Efna2	Chr 10_40	23.6	5.3	1.0	Me	
Sema5a	Chr 15_18	120.3	19.1	1.8	Me	
Aire	Chr 10_40	18.0	8.6	1.2	N, C	Tc, Tl
Fgf8	Chr 19_49	24.7	11.1	1.8	E	
Snrpd2	AA*	13.6	13.4	3.3	N	
Hmgn2	AA	9.4	85.7	2.2	N, C	
Mcrs1	AA	51.7	45.5	3.2	N	
Hnrpa2b1	AA	32.5	19.5	2.1		
Hars	AA	57.4	104.9	4.8	C	Tl
Rpo1−3	AA*	15.1	6.4	4.2		

Table 1. Continued

gene symbol	source[a]	M_w (kDa)	MRL/lpr[b]	NMS[b]	Gene Ontology[c] cellular location	Gene Ontology[c] biological function/process
Hars2	AA*	23.4	7.3	1.6	C, Mi	Tl
Hspca	AA	84.8	5.9	3.1		
Vtn	AA	54.8	5.8	1.6	E	
Snrpd3	AA*	13.9	10.2	2.8	N, C	
Hmgn1	AA*	10.1	35.6	4.5	N, C	Tc
Rnps1	AA	40.8	26.0	1.4	N, C	
Fbl	AA	34.2	24.9	1.9	N	
Npm1	AA	32.6	12.6	1.1	N, C	K
Top3b	AA*	96.9	18.9	2.6		
Coil	AA	62.2	9.8	1.6	N	
Casp8	AA	55.4	27.5	2.8	N, C	P
Ybx1	AA	35.7	27.8	4.7	N, C	Tc
Srpk1	AA	73.1	17.7	3.8	N, C	K
Rpa1	AA	71.4	36.6	3.8	N	
Car9	AA*	47.3	8.9	1.5	Me	
Sag	AA	44.9	11.9	2.2		
Dnahc8	AA	122.1	9.2	1.6	C	
Top3a	AA*	107.0	13.1	2.0		
Fbn2	AA	56.6	5.9	1.4	E	

[a] The source of selected gene done by symbol, is as follows: Chr 10_40, genetic loci on chromosome 10_40 cM; Chr 15_18, genetic loci on chromosome 15_18 cM; Chr 19_49, genetic loci on chromosome 19_49 cM; AA, well-known autoantigen; AA*, well-known autoantigen homologue. [b] Relative luminescence signals. [c] According to Gene Ontology (GO) Database (http://www.geneontology.org/), the proteins were classified by cellular localization and biological function/process, is as follows: Me, Membrane (GO:0016020); N, Nucleus (GO:0005634); C, Cytoplasm (GO:0005737); E, Extracellular region (GO:0005576); Mi, Mitochondrion (GO:0005739); K, Kinase activity (GO:0016301); P, Peptidase activity (GO:0008233); U, Ubiquitin (GO:0005551); Tl, Translation (GO:0006412); Tc, Transcription (GO:0006350). [d] Hhex, lane1; Sgta, lane3; Slc1a6, lane4 in Figure 4.

reactive autoantigen proteins. Interestingly, these loci were reported as the susceptibility loci of arthritis. Furthermore, according to Gene Ontology (GO) Database (http://www.geneontology.org/), 73 (76%) of the proteins were classified by cellular localization (Figure 3E) and 25 (26%) classified by biological function/process (Figure 3F). The annotated proteins found were classified as localized with Membrane (22%), Membrane/Cytoplasm (4%), Extracellular space (7%), Nucleus (13%), Nucleus/Cytoplasm (13%), Cytoplasm (7%) and Mitochondrion (2%). Also, the annotated proteins were involved in diverse biological functions/processes such as Kinase activity (8%), Kinase activity/peptidase activity (1%), transcription (8%), Transcription/Translation (1%), Translation (3%), Ubiquitin/Translation (1%) and Peptidase activity (3%). Data analysis showed that 26 and 25 proteins were annotated in localization of nucleus and cytoplasm respectively (Figure 3E, Table 1), and that 9 and 9 proteins were related to cellular events of protein phosphorylation and transcription, respectively (Figure 3F, Table 1). Many nuclear proteins were reported as autoantigens.[2] Interestingly, localization of 38 (39.6%) antigen proteins reacting with antibodies in MRL/lpr mouse sera was annotated in membrane and/or extracellular space. These results suggest that the wheat cell-free system is a viable platform to study folded membrane proteins that function as antigens. The data analysis suggests that MRL/lpr autoantigen proteins are represented by a wide variety of biological functions localized in whole cells, rather than just nuclear proteins. Taken together, these results indicate that the BPL-based screening method would be useful for identification of autoantigen proteins.

Validation of Identified Autoantigen Proteins by Immunoblotting and Immunoprecipitation. Recent reports have mentioned the possibility that autoantibodies may react with conformational epitopes.[29−31] These data were obtained by liquid phase immunoprecipitation assays using recombinant proteins.[32,33] Under these situations, autoantigen proteins we found were analyzed by immunoblotting and immunoprecipitation. For this analysis, six proteins were randomly selected (see legend in Figure 4). Immunoblot analysis showed that three proteins reacted with MRL/lpr mouse sera (Lanes 2, 5, and 6 in Figure 4A). Two of these three proteins, LmnB2 (Lane 5) and topoisomerase II alpha (Top2a) (Lane 6), have been well characterized as autoantigen proteins so far.[22,34] Also, six of our identified autoantigen proteins were not detected by immunoblot analysis in the sera of NMS (data not shown). Interestingly, immunoprecipitation analysis revealed antigenicity of all six autoantigen proteins (Figure 4B, C), whereas two proteins randomly selected from nonautoantigen proteins, serving as a negative control, did not show significant reaction to the sera from MRL/lpr mice by both immunoblot analysis and immunoprecipitation (Lanes 7 and 8 in Figure 4A, B). These results suggest that the BPL-based screening method may be useful for identification of autoantigen proteins reacting with autoantibodies recognizing conformational epitopes.

Discussion

To address high-throughput protein production, we have utilized our wheat germ high-throughput protein synthesis system,[10,16] which can produce large numbers of recombinant proteins using a fully automated robot.[19] To create a library of target autoantigen proteins, full-length human and mouse cDNA resources were provided by the Mammalian Gene Collection (MGC) clones (Mammalian Gene Collection Program, http://mgc.nci.nih.gov/) and FANTOM.[27,28] Since the full-length cDNA was provided in plasmids, no additional time-consuming cloning steps were needed for the synthesis of linear DNA templates by PCR for direct entry into the cell-free based protein production system. Additionally, researchers can select and use any appropriate peptide tag for downstream applications, like a bls used in this study, owing to the ease of template construction. In fact, given the advantages of the gateway system and PCR, a recent publication reported successful production of 13 000 His-tagged human proteins by the wheat cell-free system using full-length cDNA resources.[12] Furthermore, because protein purification is a time-consuming-step, an assay system with no purification requirement could dramatically increase the throughput. For that, a specific

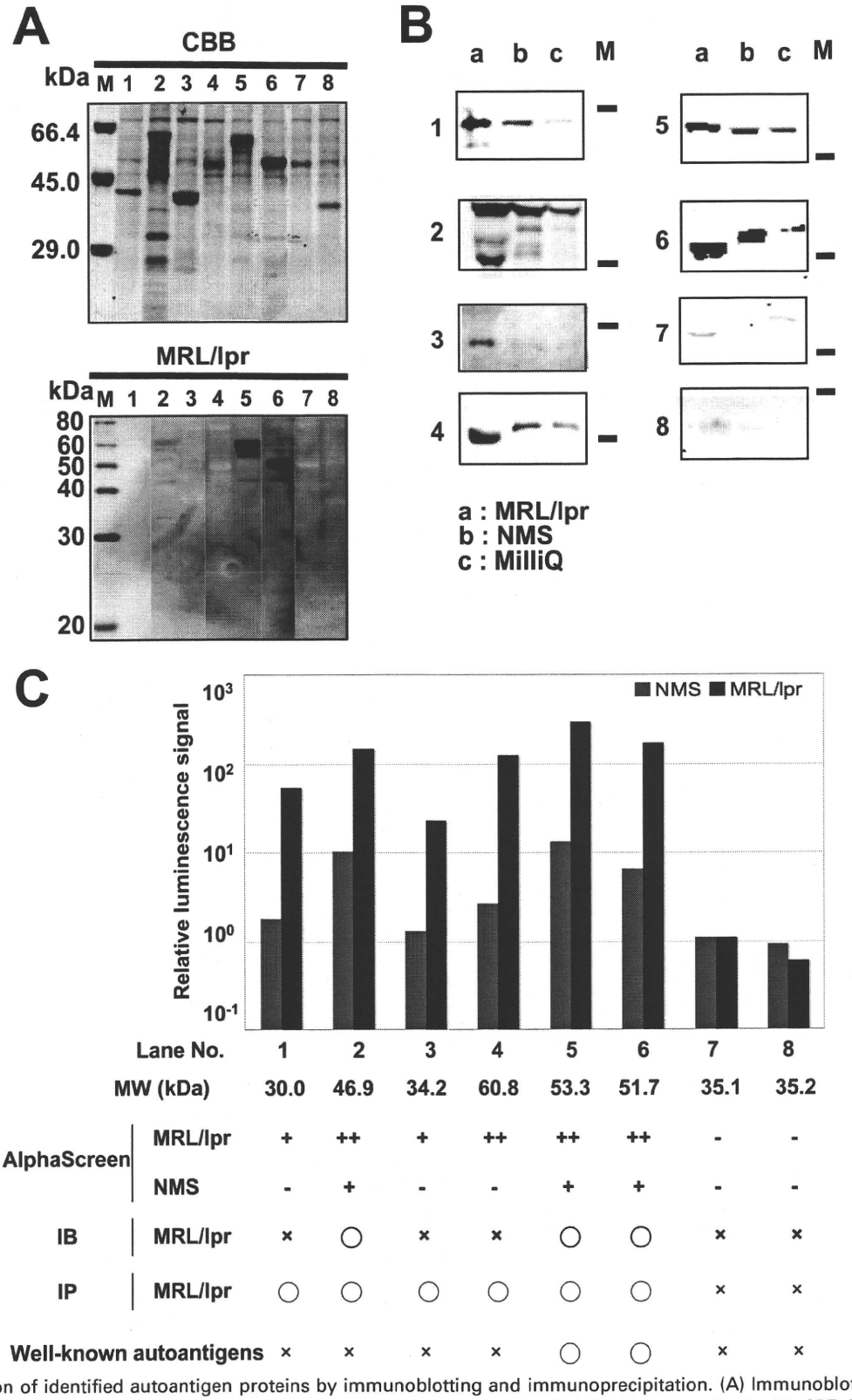

Figure 4. Detection of identified autoantigen proteins by immunoblotting and immunoprecipitation. (A) Immunoblotting analysis by using recombinant proteins. Purified recombinant proteins were separated by SDS-PAGE and stained with CBB (Upper). Purified recombinant proteins were reacted with serum from MRL/lpr mouse (Lower). (B) Immunoprecipitation analysis using recombinant proteins. Translation mixtures expressing biotinylated proteins were incubated with 1 μL of undiluted serum overnight at 4 °C. Immobilized Protein A sepharose was added to each sample, and incubated for 60 min at 4 °C. After washing, proteins were separated by SDS-PAGE, followed by immunoblotting with Alexa488-STA. M indicates a 45 kDa protein molecular weight marker. (C) Whole data of randomly selected proteins. IB, Immunoblotting; IP, Immunoprecipitation. Relative luminescence signal, $10^2 \leq ++$; $5 \leq + < 10^2$; $- < 5$. (A, B, C) Lane 1, Hhex; Lane 2, Tdg; Lane 3, Sgta; Lane 4, Slc1a6; Lane 5, Lmnb2; Lane 6, Top2a; Lane 7, Cs; Lane 8, Car4. Lane 7 and 8 were negative controls. Detailed information on individual proteins was indicated in Supplementary Table 1 (Supporting Information).

protein has to be clearly recognized in a homogeneous condition. In this study, we selected biotin as our target protein label due to the highly specific binding of biotin-streptavidin. Commonly, biotinylated proteins are produced via NHS ester-activated biotins. However, this technique requires laborious purification to remove any nonreacted biotin reagent in the reaction mixture. Therefore, we used a BirA biotin-ligase-based labeling system. By addition of BirA and biotin to the wheat cell-free system, highly specific biotin-labeling is available and the biotinylated proteins can be directly used for assaying[13,15,35] without further purification. Taken together, the biotinylated protein library produced by the wheat cell-free system is suitable for autoantigen screening.

Several autoantigen screening methods such as SERPA, SEREX and protein microarray are currently widely used for identification of autoantigen proteins, each of which has inherent limitations. In this study, we demonstrated improved methodologies that overcome the aforementioned limitations using a wheat cell-free based BPL and luminescence assay that allow detection of autoantigen proteins with autoantibodies in sera. The BPL-based screening revealed that specific antibody interaction were detected at subpicogram scale, with a linear response over a 1000-fold range, and appear to be more sensitive than conventional method, such as ELISA.[6,36] It should be noted that protein microarray could also detect autoantigen at picogram scale, in the linear fashion over a 1000-fold range.[6] While the detection sensitivity of the BPL-based autoantigen protein screening method might be equivalent to microarray based autoantigen protein screening, the folded state of the autoantigen proteins differs. The reports which autoantibodies would recognize conformational epitopes[29,30] might contain an important implication for screening of autoantigen proteins. Although conventional methods use denatured or unfolded proteins, such as dehydrated or detergent-treated proteins, the BPL-based method tested in this study better represents the folded, native form as all procedures are carried out in the solution phase without dehydration or detergent treatment. In addition, the BPL-based screening method using serum dilutions of 1:10 000 could produce high luminescent signal in 25 μL of reaction volume (Figure 2C). Thus, 50 μL of serum would be sufficient to screen 20 000 kinds of human proteins.

Autoimmune diseases were thought to be a complex of both genetic and nongenetic factors influencing susceptibility, severity and response to therapies.[37] Twin and family studies suggest that approximately 60% of susceptibility is due to genetic factors and genes within the HLA locus, particularly HLA-DRB1, which accounts for almost half of the genetic component of susceptibility.[37] Also, genetic analyses identified that other susceptibility locus of RA, SLE, and so on.[38] In this study, we screened proteins encoded by genes on an autoimmune susceptibility loci,[26] and 71 out of 111 clones (Table 1 and Supplementary Table 1, Supporting Information) localized on the chromosomes 10, 15 and 19[26] were found as new autoantigen proteins reacting with the sera of MRL/lpr mice. Additionally, the Gene Ontology (GO) Database may be extremely useful for the screening of autoantigen protein. For example, based on data from the GO Database, localization of 38 (39.6%) autoantigen proteins out of 96 MRL/lpr autoantigen proteins were annotated in membrane and/or extracellular space (Figure 3E). These results suggest that a specific protein library focused on the human autoimmune susceptibility loci and membrane proteins or extracellular spaces classified according to GO Database may be a good target for screening of autoantigen proteins.

A key obstacle for robust genome-wide screening has been experimentally simple techniques and automated technology. The BPL-based screening method is one of the simplest approaches for identification of autoantigen proteins, because all experimental processes, including construction of DNA templates, and interaction and detection of antigen−autoantibodies reactions, were reduced to mixing steps. Synthesis of the biotinylated protein library was accomplished using a fully automated robot,[19] and the biotinylated proteins can be used in subsequent screening steps without purification. The method described here can be used in developed for use in 96, 384 (Figure 3A) or 1536-well microtiter-plate format through the use of appropriate automated liquid handling robots. Therefore this method is suitable for development of a genome-wide screening platform. In conclusion, the BPL-based screening method has a high potential for identification of autoantigen proteins in human autoimmune diseases.

Abbreviations: Alexa488-STA, streptavidin Alexa Fluor 488 conjugate; NMS, normal mouse sera; SEREX, serological expression cloning; SERPA, serological proteome analysis; bls, biotin ligation site; DHFR, dihydrofolate reductase; Lmnb2, lamin B2; Hars, histidyl-tRNA synthetase; Top2a, topoisomerase II alpha; Hhex, hematopoietically expressed homeobox; Tdg, thymine DNA glycosylase; Sgta, small glutamine-rich tetratricopeptide repeat (TPR)-containing, alpha; Slc1a6, solute carrier family 1 (high affinity aspartate/glutamate transporter), member 6; Cs, citrate synthase; Car4, carbonic anhydrase 4; BPL, biotinylated protein library; FANTOM, functional annotation of mouse; CBB, coomassie brilliant blue; RF, rheumatoid factor; hnRNP, heterogeneous nuclear ribonucleoprotein; Sm, Smith; GO, Gene Ontology; NHS, *N*-hydroxysuccinimide; RA, rheumatoid arthritis; SLE, systemic lupus erythematosus; MRL/lpr, MRL/Mp-*lpr/lpr*.

Acknowledgment. This work was partially supported by the Special Coordination Funds for Promoting Science and Technology by the Ministry of Education, Culture, Sports, Science and Technology, Japan (T.S. and Y.E.). We thank Michael Andy Goren and Dr. Akira Nozawa for proofreading this manuscript.

Supporting Information Available: Supplementary Table 1: List of selected 226 mouse genes and primer sequences used in this study. This material is available free of charge via the Internet at http://pubs.acs.org.

References

(1) Davidson, A.; Diamond, B. *N. Engl. J. Med.* **2001**, *345* (5), 340–50.
(2) von Mühlen, C.; Tan, E. *Semin. Arthritis Rheum.* **1995**, *24* (5), 323–58.
(3) Mewar, D.; Wilson, A. *Biomed. Pharmacother.* **2006**, *60* (10), 648–55.
(4) Gunawardana, C.; Diamandis, E. *Cancer Lett.* **2007**, *249* (1), 110–9.
(5) Anderson, K.; Ramachandran, N.; Wong, J.; Raphael, J.; Hainsworth, E.; Demirkan, G.; Cramer, D.; Aronzon, D.; Hodi, F.; Harris, L.; et al. *J. Proteome Res.* **2008**, *7* (4), 1490–9.
(6) Robinson, W.; DiGennaro, C.; Hueber, W.; Haab, B.; Kamachi, M.; Dean, E.; Fournel, S.; Fong, D.; Genovese, M.; de Vegvar, H.; et al. *Nat. Med.* **2002**, *8* (3), 295–301.
(7) Hudson, M.; Pozdnyakova, I.; Haines, K.; Mor, G.; Snyder, M. *Proc. Natl. Acad. Sci. U.S.A.* **2007**, *104* (44), 17494–9.
(8) Sheridan, C. *Nat. Biotechnol.* **2005**, *23* (1), 3–4.
(9) Zhu, H.; Snyder, M. *Curr. Opin. Chem. Biol.* **2003**, *7* (1), 55–63.

(10) Sawasaki, T.; Ogasawara, T.; Morishita, R.; Endo, Y. *Proc. Natl. Acad. Sci. U.S.A.* **2002**, *99* (23), 14652–7.
(11) Endo, Y.; Sawasaki, T. *Methods Mol. Biol.* **2005**, *310*, 145–67.
(12) Goshima, N.; Kawamura, Y.; Fukumoto, A.; Miura, A.; Honma, R.; Satoh, R.; Wakamatsu, A.; Yamamoto, J.; Kimura, K.; Nishikawa, T.; et al. *Nat. Methods* **2008**, *5* (12), 1011–7.
(13) Sawasaki, T.; Kamura, N.; Matsunaga, S.; Saeki, M.; Tsuchimochi, M.; Morishita, R.; Endo, Y. *FEBS Lett.* **2008**, *582* (2), 221–8.
(14) Beaudet, L.; Bédard, J.; Breton, B.; Mercuri, R.; Budarf, M. *Genome Res.* **2001**, *11* (4), 600–8.
(15) Takahashi, H.; Nozawa, A.; Seki, M.; Shinozaki, K.; Endo, Y.; Sawasaki, T. *BMC Plant Biol.* **2009**, *9*, 39.
(16) Madin, K.; Sawasaki, T.; Ogasawara, T.; Endo, Y. *Proc. Natl. Acad. Sci. U.S.A.* **2000**, *97* (2), 559–64.
(17) Sawasaki, T.; Morishita, R.; Gouda, M.; Endo, Y. *Methods Mol. Biol.* **2007**, *375*, 95–106.
(18) Sawasaki, T.; Hasegawa, Y.; Tsuchimochi, M.; Kamura, N.; Ogasawara, T.; Kuroita, T.; Endo, Y. *FEBS Lett.* **2002**, *514* (1), 102–5.
(19) Sawasaki, T.; Gouda, M.; Kawasaki, T.; Tsuboi, T.; Tozawa, Y.; Takai, K.; Endo, Y. *Methods Mol. Biol.* **2005**, *310*, 131–44.
(20) Stephen, C.; Helminen, P.; Lane, D. *J. Mol. Biol.* **1995**, *248* (1), 58–78.
(21) Miller, F.; Waite, K.; Biswas, T.; Plotz, P. *Proc. Natl. Acad. Sci. U.S.A.* **1990**, *87* (24), 9933–7.
(22) Brito, J.; Biamonti, G.; Caporali, R.; Montecucco, C. *J. Immunol.* **1994**, *153* (5), 2268–77.
(23) Theofilopoulos, A.; Dixon, F. *Adv. Immunol.* **1985**, *37*, 269–390.
(24) Spirin, A. *Trends Biotechnol.* **2004**, *22* (10), 538–45.
(25) Endo, Y.; Sawasaki, T. *Biotechnol. Adv.* **2003**, *21* (8), 695–713.
(26) Nose, M. *Allergol. Int.* **2007**, *56* (2), 79–86.
(27) Okazaki, Y.; Furuno, M.; Kasukawa, T.; Adachi, J.; Bono, H.; Kondo, S.; Nikaido, I.; Osato, N.; Saito, R.; Suzuki, H.; et al. *Nature* **2002**, *420* (6915), 563–73.
(28) Carninci, P.; Kasukawa, T.; Katayama, S.; Gough, J.; Frith, M.; Maeda, N.; Oyama, R.; Ravasi, T.; Lenhard, B.; Wells, C.; et al. *Science* **2005**, *309* (5740), 1559–63.
(29) Xie, H.; Zhang, B.; Matsumoto, Y.; Li, Q.; Notkins, A.; Lan, M. *J. Immunol.* **1997**, *159* (7), 3662–7.
(30) Tuomi, T.; Rowley, M.; Knowles, W.; Chen, Q.; McAnally, T.; Zimmet, P.; Mackay, I. *Clin. Immunol. Immunopathol.* **1994**, *71* (1), 53–9.
(31) Mackay, I.; Rowley, M. *Autoimmun. Rev.* **2004**, *3* (7–8), 487–92.
(32) Lan, M.; Wasserfall, C.; Maclaren, N.; Notkins, A. *Proc. Natl. Acad. Sci. U.S.A.* **1996**, *93* (13), 6367–70.
(33) Grubin, C.; Daniels, T.; Toivola, B.; Landin-Olsson, M.; Hagopian, W.; Li, L.; Karlsen, A.; Boel, E.; Michelsen, B.; Lernmark, A. *Diabetologia* **1994**, *37* (4), 344–50.
(34) Chang, Y. H.; Shiau, M. Y.; Tsai, S. T.; Lan, M. S. *Biochem. Biophys. Res. Commun.* **2004**, *320* (3), 802–9.
(35) Masaoka, T.; Nishi, M.; Ryo, A.; Endo, Y.; Sawasaki, T. *FEBS Lett.* **2008**, *582* (13), 1795–801.
(36) Quintana, F. J.; Farez, M. F.; Viglietta, V.; Iglesias, A. H.; Merbl, Y.; Izquierdo, G.; Lucas, M.; Basso, A. S.; Khoury, S. J.; Lucchinetti, C. F.; Cohen, I. R.; Weiner, H. L. *Proc. Natl. Acad. Sci. U.S.A.* **2008**, *105* (48), 18889–94.
(37) Wordsworth, P.; Bell, J. *Ann. Rheum. Dis.* **1991**, *50* (6), 343–6.
(38) Cornélis, F.; Fauré, S.; Martinez, M.; Prud'homme, J.; Fritz, P.; Dib, C.; Alves, H.; Barrera, P.; de Vries, N.; Balsa, A.; et al. *Proc. Natl. Acad. Sci. U.S.A.* **1998**, *95* (18), 10746–50.

PR9010553

Citation: Cell Death and Disease (2010) e89; doi:10.1038/cddis.2010.65

www.nature.com/cddis

Characterization of a caspase-3-substrate kinome using an N- and C-terminally tagged protein kinase library produced by a cell-free system

D Tadokoro[1], S Takahama[2], K Shimizu[1], S Hayashi[1], Y Endo*[,1,2,3] and T Sawasaki*[,1,2,3]

Caspase-3 (CASP3) cleaves many proteins including protein kinases (PKs). Understanding the relationship(s) between CASP3 and its PK substrates is necessary to delineate the apoptosis signaling cascades that are controlled by CASP3 activity. We report herein the characterization of a CASP3-substrate kinome using a simple cell-free system to synthesize a library that contained 304 PKs tagged at their N- and C-termini (NCtagged PKs) and a luminescence assay to report CASP3 cleavage events. Forty-three PKs, including 30 newly identified PKs, were found to be CASP3 substrates, and 28 cleavage sites in 23 PKs were determined. Interestingly, 16 out of the 23 PKs have cleavage sites within 60 residues of their N- or C-termini. Furthermore, 29 of the PKs were cleaved in apoptotic cells, including five that were cleaved near their termini *in vitro*. In total, approximately 14% of the PKs tested were CASP3 substrates, suggesting that CASP3 cleavage of PKs may be a signature event in apoptotic-signaling cascades. This proteolytic assay method would identify other protease substrates.

Cell Death and Disease (2010) **1**, e89; doi:10.1038/cddis.2010.65; published online 28 October 2010
Subject Category: Immunity

On the basis of the corresponding genetic sequences, >500 human and mouse proteolytic enzymes have been predicted.[1] This number is comparable with that found for protein kinases (PKs), which are the main signal-transduction enzymes.[2,3] Proteases are involved in the maturation, localization, stabilization, and complex formation of proteins, and in many biological processes, for example, normal development,[4,5] cancer,[6,7] infectious diseases,[8] and cell death.[9] Therefore, it is important to be able to identify protease substrates using simple assays.

Apoptosis requires the action of many different proteins that participate in apoptotic cell-signaling pathways.[10] Caspases and PKs are critical components of growth and apoptosis signaling pathways.[2,10] Large-scale analyses of the biological networks involving PKs and caspases are vital for the elucidation of apoptosis signaling pathways. Recent whole-cell proteomic studies that used mass spectrometry attempted to identify substrates of caspases that are involved in apoptosis and have shown that the percentage of PKs found as caspase substrates during apoptosis is 3–6% of ~300.[11,12] However, cellular protein expression levels may have biased the results.[13] Furthermore, it is difficult to identify specific pairs of proteases and substrates because numerous cleavage events occur simultaneously in cells. Therefore, an *in vitro* approach that could identify specific proteases and their corresponding substrates would complement cell-based approaches. A diagram, derived from a comprehensive *in vitro* study, that illustrates the relationships between caspases and their PK substrates would help clarify the signal-transduction events that occur during apoptosis.

A collection of recombinant proteins, that is, a protein library, is needed to screen a large number of protein substrates. In addition, to screen a protein library comprehensively two *in vitro* high-throughput methods – one for protein synthesis and one for the detection of the targeted biochemical reaction – are required. Recently, we developed an automated protein synthesis system that uses a wheat cell-free system.[14–16] Using this system, we were able to synthesize many human and Arabidopsis PKs.[17,18] Recent work by others suggested that the wheat cell-free system could produce 13 364 human proteins, which, because of the large number of proteins involved, represents an *in vitro*-expressed proteome.[19] We also recently developed a method to label monobiotin proteins that had been synthesized in the wheat cell-free system.[20] These monobiotin-labeled proteins were then used directly – without purification – to detect protein ubiquitination[21] and an autoantibody in the serum.[22] As the procedures used with many commercially available detection kits depend on biotin–streptavidin interactions, our purification-free, synthesis/biotin-labeling method provides a simple and highly specific system that can be used for biochemical analyses.

Caspase-3 (CASP3) cleaves many different proteins,[23,24] and its action *in vivo* irreversibly induces apoptosis. For the study reported herein, we delineated a CASP3-substrate kinome using a simple luminescent-based detection method

[1]Cell-Free Science and Technology Research Center, Ehime University, Matsuyama, Ehime, Japan; [2]The Venture Business Laboratory, Ehime University, Matsuyama, Ehime, Japan and [3]RIKEN Genomic Sciences Center, Tsurumi, Yokohama, Japan
*Corresponding authors: T Sawasaki or Y Endo, Cell-Free Science and Technology Research Center, Ehime University, 3 Bunkyo-cho, Matsuyama, Ehime 790-8577, Japan. Tel: +81 89 927 8530; Fax: +81 89 927 9941; E-mail: sawasaki@eng.ehime-u.ac.jp or Tel: +81 89 927 9936; Fax: +81 89 927 9941; E-mail: yendo@eng.ehime-u.ac.jp
Keywords: caspase; protein kinases; apoptosis; cell-free protein synthesis; protein library
Abbreviations: CASP3, caspase 3; PK, protein kinase; NCtagged, N- and C-terminally tagged; TD, terminal detection
Received 10.6.10; revised 31.8.10; accepted 15.9.10; Edited by A Finazzi-Agró

to screen an N- and C-terminally tagged (NCtagged) PK library produced in the wheat cell-free system. This comprehensive characterization of a CASP3-substrate kinome is a resource that can be used to understand the roles of PKs in apoptosis.

Results

Generation of an NCtagged PK library used to identify CASP3 PK substrates. To identify PKs that are substrates of CASP3, we first made a library consisting of 248 human and 56 mouse PKs (Supplementary Table S1). The nucleotide sequences for the Flag-tag and the biotin ligation site (bls) were added upstream and downstream, respectively, of the *PK* open-reading frame by PCR incorporation of Gateway recombination tags. Each PCR product (attB1-Flag-*PK*-bls-attB2) was inserted into a pDONR221 vector using the Gateway BP Clonase II system (upper panel, Figure 1). The Flag-*PK*-bls nucleotide sequences from the *Escherichia coli* cultures were used without purification to construct, by split-primer PCR, the DNA templates for protein synthesis.[14] The NCtagged PK library (304 PKs) was produced using an automated protein synthesizer (GenDecoder 1000; CellFree Sciences Co., Ltd., Matsuyama, Japan), with biotin and biotin ligase added into the synthesis mixtures for monobiotin labeling at the bls.[20,21] That the members of the protein library were NCtagged was confirmed by immunoblotting with anti-Flag antibodies and Alexa488-labeled streptavidin.

To assess the suitability of the designed PKs to act as CASP3 substrates, we used NCtagged p21-activated kinase 2 (PAK2), which is a known CASP3 substrate,[25] as the test case. The biotinylated NCtagged-PAK2 (Flag-PAK2-bls~biotin) was treated with CASP3 and cleavage of PAK2 was confirmed by immunoblotting with Alexa488-conjugated streptavidin (Figure 2a). In addition, the cleavage site ($_{319}$DELD↓S_{323}), determined by amino-acid sequencing, was found to be the same as that reported previously.[25] (The arrow indicates the hydrolytic bond.)

A luminescent assay to detect PK substrates of CASP3. A schematic of the assay used to monitor cleavage of the NCtagged PKs by CASP3 is shown in Figure 1. The PK construct is first incubated with CASP3. If the construct contains a sequence that can be cleaved by CASP3, cleavage occurs. Acceptor and donor beads are then added. The Flag-tag binds a protein A-conjugated acceptor bead via an anti-Flag antibody, and the biotin bound to the C-terminus of the PK construct binds a streptavidin-conjugated donor bead. If an acceptor bead is in close contact with the donor bead, as is the case when the construct is not a CASP3 substrate and both beads are therefore bound intramolecularly, the system luminesces. However, if CASP3 had cleaved the NCtagged PK, luminescence is suppressed because the beads are no longer in close contact. As a proof-of-concept experiment, cleavage of the test PK, NCtagged PAK2, was assessed

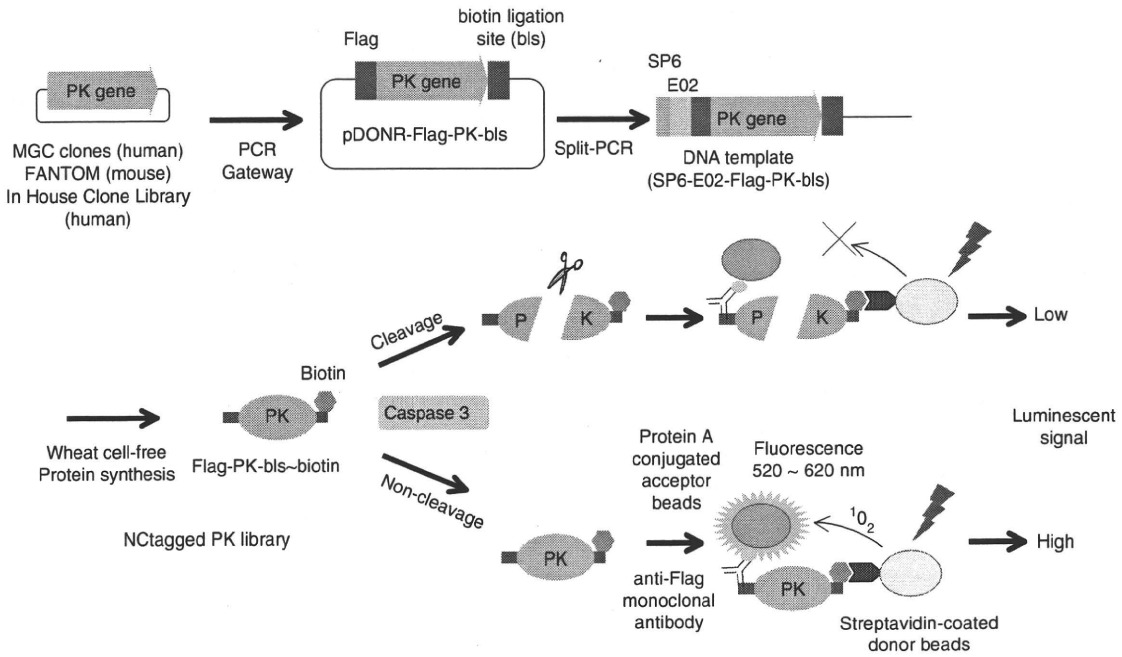

Figure 1 Schematics of the DNA template construction and the CASP3-substrate-screening assay. *Protein kinase* (*PK*) genes were obtained from the human MGC and mouse FANTOM libraries, and from a library of *PK* genes that we had cloned. The *PK* genes were PCR amplified with the Flag and the biotin ligation site (bls) tags added to the upstream and downstream ends, respectively. The modified genes were each inserted into a Gateway pDONR221 vector (pDONR-Flag-PK-bls) and DNA templates (SP6-E02-Flag-*PK*-bls) were constructed by split-primer PCR and then expressed in the wheat cell-free protein synthesis system that included biotin ligase and D-biotin to give Flag-PK-bls~biotin constructs. The Flag and biotin tags were bound to protein A-conjugated acceptor beads via an anti-Flag antibody and streptavidin-conjugated donor beads, respectively. An intact complex luminesced strongly, whereas after CASP3 cleavage and dissociation of the protein fragments, the luminescence was abolished or reduced

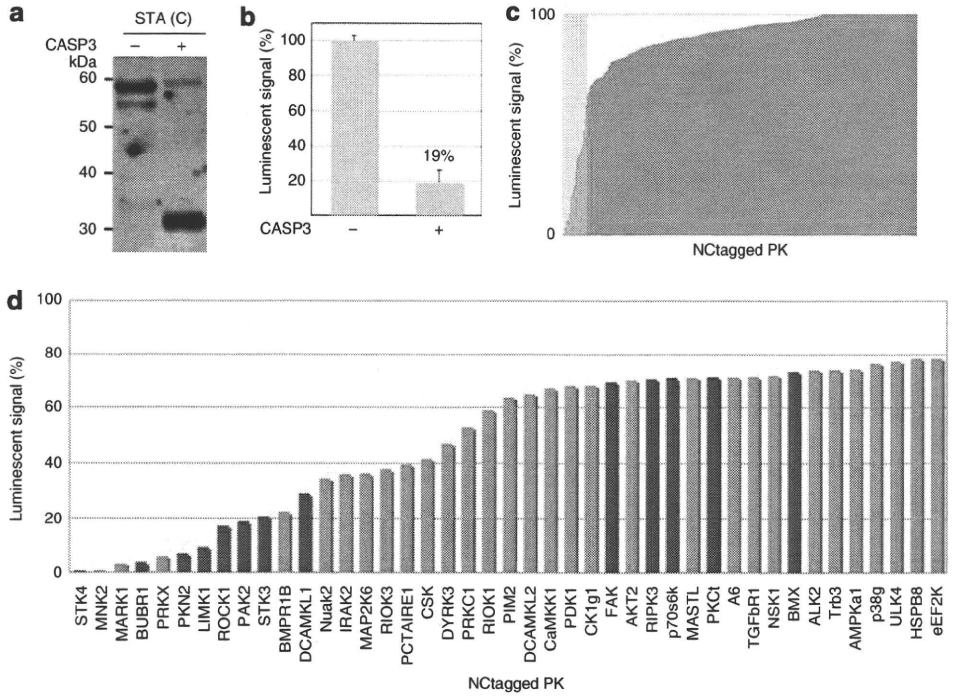

Figure 2 Screening of CASP3-cleaved PK substrates from the NCtagged PK library. (**a**) Immunoblot of NCtagged PAK2 that had been incubated in the presence (+) or absence (−) of CASP3. Alexa488-labeled streptavidin (STA(C)) was used for detection. (**b**) Detection of CASP3-cleaved NCtagged PAK2 using the AlphaScreen system. The luminescence for the control (no CASP3) was set to 100%. The value of 19% indicated that most of the NCtagged PAK2 was cleaved by CASP3. Each value is the mean of three independent experiments, and the uncertainty is reported as the standard deviation. (**c**) Luminescent signals remaining after *in vitro* CASP3 treatment of NCtagged PKs that had been synthesized in the wheat cell-free system. The *x* axis lists the NCtagged PKs in ascending order of their luminescent signals after CASP3 treatment. (**d**) NCtagged PKs that returned luminescent signals of <78% of the control values. The plot contains the data of (**c**) within the green rectangle. Red bars are for PKs that were known to be substrates of CASP3 before this report

using this system. CASP3 treatment decreased the luminescent signal to 19 ± 7% that of the control (no CASP3; Figure 2b). Therefore, the system could detect CASP3 cleavage and can replace conventional immunoblotting procedures.

Screening of the CASP3-substrate kinome. Using the luminescent system, 304 NCtagged PKs were screened. The level of luminescence after CASP3 treatment is reported as the percentage of the corresponding control (no CASP3; Figure 2c and d). Thirteen of the NCtagged PKs for which luminescence was low after CASP3 treatment are known CASP3 substrates.[23,24,26] The smallest and largest luminescent values were for STK4 (1%) and BMX (73%), respectively; we therefore examined the physical states of the PKs that had been treated with CASP3 and had associated luminescence values of ~80% by immunoblotting with anti-Flag antibodies and Alexa488-streptavidin to detect the N- and C-termini of the NCtagged PKs, respectively. This 'terminal detection' (TD) immunoblot assay identified 43 NCtagged PKs that had been cleaved (Supplementary Table S1). In addition to the 13 PKs that were known to be CASP3 substrates, 30 previously unidentified PK that were substrates of CASP3 were found (Figure 3 and Table 1). In addition, because the apparent molecular weights of the N- and C-terminal fragments could be estimated from their positions in the TD immunoblot, the CASP3 cleavage sites could be predicted (red arrowheads, Figure 3). For MASTL, the signal on the immunoblot with Alexa488-conjugated streptavidin was not detectable, probably indicating that the efficiency of biotinylation in MASTL proteins might be too low to detect for the immunoblot. Luminescent signal of this clone was also very low (see Supplementary Table S1).

A comparison of the luminescent and immunoblot data correlated a luminescent signal of <78% with a positive immunoblot result. Forty-eight PK constructs with luminescent signals >78% were tested and returned negative immunoblot results (Supplementary Table S1). Therefore, a luminescent signal of ~78% is the apparent divisor between PKs that can be cleaved by CASP3 and those that cannot be cleaved.

***In vivo* identification of the PKs that were identified as CASP3 substrates by the luminescent assay.** We investigated whether the newly identified PKs that were substrates of CASP3 were cleaved in HeLa cells that had been induced to undergo apoptosis by TNFα plus cycloheximide (TNFα)[27] or anti-Fas antibody (anti-Fas).[28] The genes encoding these PKs were each inserted into the transfection vector, pDEST26, using the Gateway system and expressed as $(His)_6$-PK-Flag constructs. We were able to detect all expressed PK constructs, except DYRK3, by immunoblotting with anti-$(His)_6$ or anti-Flag antibodies.

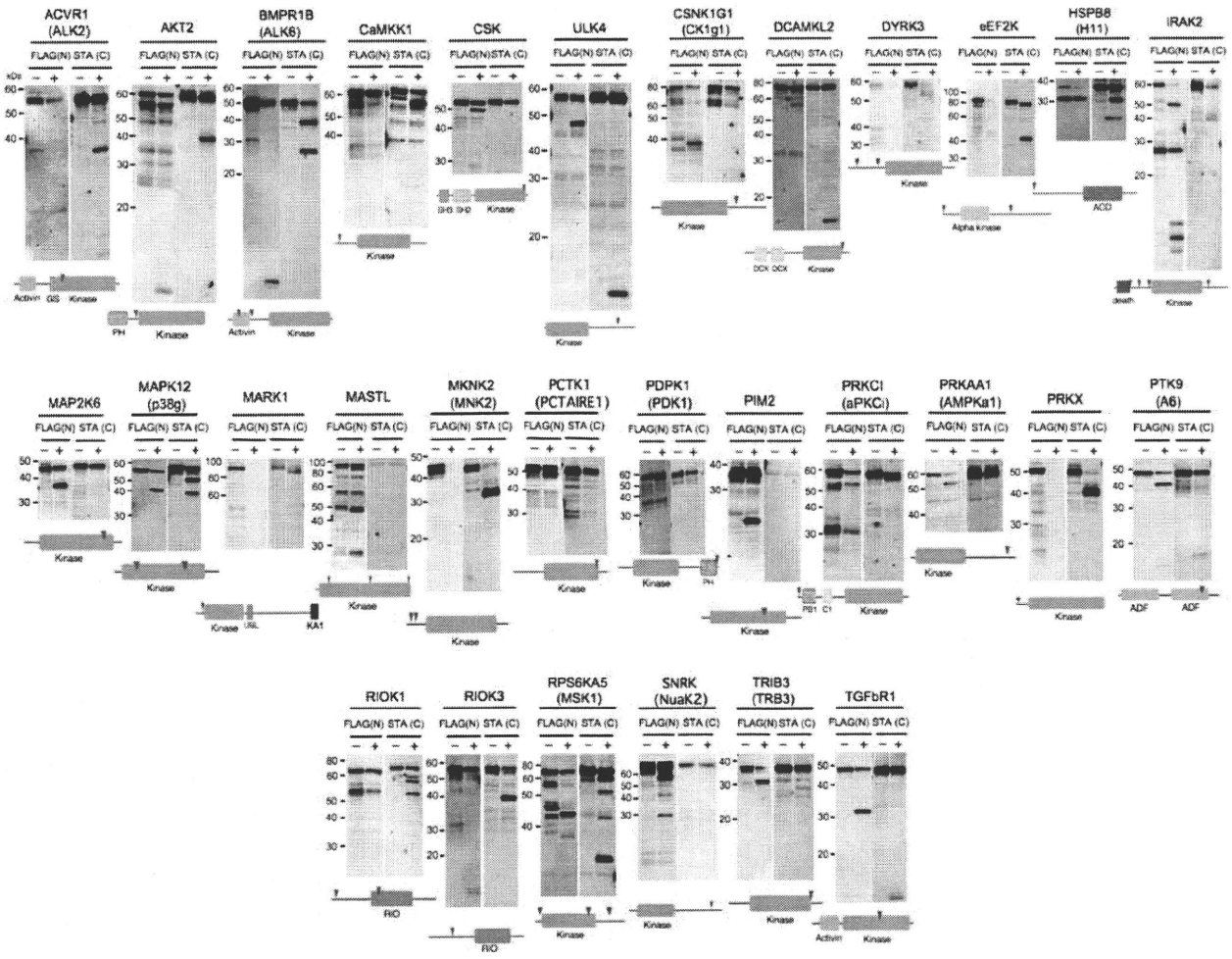

Figure 3 *In vitro* cleavage of NCtagged PKs by CASP3. The NCtagged PKs that had been incubated in the presence (+) or absence (−) of CASP3 and their cleavage products were detected using anti-Flag antibodies (FLAG(N)) and Alexa488-conjugated streptavidin (STA(C)), which bound to the N- and C-termini of the PK constructs, respectively. The cartoons of the proteins that are under the lanes show the locations of the conserved domains (colored boxes) and the predicted cleavage sites (red arrowheads). The conserved domains that are found in the Conserved Domains Database (http://www.ncbi.nlm.nih.gov/cdd) are: ACD, alpha-crystallin domain; activin, conserved domain for activin members; ADF, actin depolymerization factor/cofilin-like domain; α-kinase, conserved kinase domain for the α-kinase family; C1, phorbol esters/diacylglycerol binding domain; DCX, doublecortin domain; death, death domain; GS, GS motif; KA1, kinase-associated domain; kinase, catalytic domain of protein kinase; PB1, Phox and Bem1p domain; PH, pleckstrin homology domain; RIO, catalytic domain of eukaryotic RIO kinase family; SH2, src homology 2 domain; SH3, src homology 3 domain; UBL, ubiquitin-like domain

Notably, they were detected as cleavage products and/or were found in smaller amounts when the cells had been induced to undergo apoptosis than when apoptosis had been inhibited by z-VAD-FMK (Figure 4a and b). Furthermore, apoptosis-induced cleavage of four endogenous PKs was found by immunoblotting with commercially available antibodies against the endogenous PKs (Figure 4c). These *in vivo* experiments validated the underlying concept of our *in vitro* cell-free system as the *in vivo* system found all of the PKs identified by the *in vitro* system.

Characterization of the CASP3 cleavage sites in the newly identified PK substrates. We characterized the CASP3 cleavage sites in the newly identified PK substrates. As the positions of the cleaved PK fragments in the TD immunoblot could be used to estimate the size of the cleaved fragments and because the antibodies could be used to identify whether the fragments were derived from the N- or C-terminal regions of the PKs, we could predict the approximate positions of the CASP3 cleavage sites (red arrowheads, Figure 3). Each NCtagged PK that was a substrate for CASP3 was synthesized in the cell-free system and purified using Streptavidin Magnesphere Paramagnetic beads. Their C-terminal fragments that bound to the beads were recovered after CASP3 cleavage and their sequences were determined. Using this approach, the cleavage sites of ACVR1, AKT2, BMPR1B, CaMKK1, HSPB8, MAPK12, MKNK2(D58), PDPK1, PRKCI, PRKX, RIOK1, RIOK3, and RPS6KA5 were determined. We then attempted to determine the cleavage sites of the remaining PKs by other methods.

The NCtagged PKs that had low biotin-labeling efficiencies and were cleaved near their C-termini were genetically modified by the addition of a glutathione-*S*-transferase (GST) fragment at their C-termini to facilitate recovery with

Table 1 Characteristics of the newly identified CASP3 PK substrates

Symbols	Kinome names	Groups	Clone origin	AA[a]	Cleavage sequence	Cleavage sites	Methods[b]	Conservation[c]	Smallest frag.[d]	*In vivo* cleavages[e]
ACVR1	ALK2	TKL	Hs	509	IASD↓M	269	NT	Yes	C240	Yes
AKT2	AKT2	AGC	Mm	481	DAMD↓Y	121	NT	Yes	N121	Yes
BMPR1B	ALK6	TKL	Hs	502	CSTD↓G	50	NT	Yes	N50	Yes
					DFVD↓G	120	NT	Yes		
CaMKK1	CaMKK1	Other	Hs	520	EEAD↓G	32	NT	Yes	N32	Yes
CSK	CSK	TK	Mm	450	DAPD↓G	409	MS	Yes	C41	Yes
CSNK1G1	CK1g1	CK1	Mm	459	VHVD↓S	343	MU	Yes	C116	Yes
eEF2K	eEF2K	Atypical	Hs	725	EGVD↓G	14	MU	Yes	N14	Yes
					DHLD↓N	430	MU	Yes		
HSPB8	H11	Atypical	Hs	196	MAD↓G	3	NT	Yes	N3	Yes
MAP2K6	MAP2K6	STE	Mm	334	DFVD↓F	289	MU	Yes	C45	Yes
MAPK12	p38g	CMGC	Hs	367	SAVD↓G	46	NT	Yes	N46	Yes
MARK1	MARK1	CAMK	Hs	795	SATD↓E	52	MU	Yes	N52	Yes
MKNK2	MNK2	CAMK	Hs	414	DQPD↓H	32	MU	No	N32	Yes
					DIPD↓A	58	NT	Yes		
PDPK1	PDK1	AGC	Hs	556	SHPD↓A	552	NT	Yes	C4	Yes
PIM2	PIM2	CAMK	Hs	334	TDFD↓G	198	MU	Yes	C113	Yes
PRKAA1	AMPKa1	CAMK	Hs	550	TSLD↓S	520	MS	Yes	C30	Yes
PRKCI	aPKCi	PKC	Hs	596	TQRD↓S	6	NT	Yes	N6	Yes
PRKX	PRKX	AGC	Hs	358	ETPD↓G	25	NT	No	N25	Yes
RIOK1	RIOK1	Atypical	Mm	568	EKDD↓I	37	NT	Yes	N37	Yes
RIOK3	RIOK3	Atypical	Hs	516	DTRD↓D	139	NT	Yes	N139	Yes
RPS6KA5	MSK1	AGC	Hs	549	DGGD↓G	20	NT	Yes	N20	Yes
					DELD↓V	344	NT	Yes		
					TEMD↓P	356	NT	Yes		
SNARK	NuaK2	CAMK	Hs	628	VSED↓S	546	MU	Yes	C82	Yes
TRIB3	TRB3	CAMK	Hs	358	VVPD↓G	338	NT	Yes	C20	Yes
ULK4	ULK4	Other	Hs	580	SQID↓S	473	MU	Yes	C107	Yes
DCAMKL2	DCAMKL2	CAMK	Hs	695	—	—	—	—	—	Yes
DYRK3	DYRK3	CMGC	Hs	568	—	—	—	—	—	ND
IRAK2	IRAK2	TKL	Mm	622	—	—	—	—	—	Yes
MASTL	MASTL	AGC	Hs	879	—	—	—	—	—	Yes
PCTK1	PCTAIRE1	CMGC	Hs	496	—	—	—	—	—	Yes
PTK9	A6	Atypical	Hs	384	—	—	—	—	—	Yes
TGFBR1	TGFBR1	TKL	Hs	426	—	—	—	—	—	Yes

Abbreviations: Hs, human clone; Mm, mouse clone; MS, mass spectroscopy; MU, mutation; ND, not determined; NT, N-terminal sequencing. [a]Length of amino acids. [b]Methods for determination of cleavage site. [c]Very similar site conserving the Asp (D) of the hydrolytic bond was found between human and mouse PKs (Yes), whereas no similar sites was done (No). [d]The smallest N (N) or C (C) fragment in the cleaved PKs. Number is the length of amino acids of the fragment. [e]Data from Figure 4.

glutathione Sepharose 4B beads after CASP3 cleavage. CASP3 cleavage of the PK-GSTs produced the same size N-terminal fragments as those of the corresponding CASP3-cleaved NCtagged PKs, indicating that the GST tags did not alter the positions of the cleavage sites. In addition, the sequences of the cleaved c-src tyrosine kinase (CSK) and AMP-activated kinase-a1 (AMPKa1) fragments were determined using MALDI/TOF-MS. Other PK constructs that were synthesized in small amounts were subjected to D→A mutagenesis to determine their cleavage sites. In total, 28 cleavage sites in 23 PKs were identified (Table 1). Identical or similar cleavage sites were found in the corresponding human and mouse PKs, except for those of PRKX (Supplementary Table S2). (Sequence analysis showed that mouse PRKX does not have the N-terminal region that is found in human PRKX.) Therefore, the CASP3-substrate kinome may be highly conserved in mammals.

We also analyzed the common sequence attributes among the 28 cleavage sites and found that CASP3 prefers the sequence, DXXD↓G (Figure 5a). The consensus PK cleavage site for CASP3 in the MEROPS database is DXXD↓X. In the NCtagged PK library, 208 of the 304 PKs contain a DXXDX sequence. However, only 33 PKs were cleaved by CASP3; therefore, to be cleaved by CASP3, the DXXDX sequence and a structural element –probably accessibility – are required.

Characterization of the newly identified PKs that were cleaved near their N- or C-termini. Interestingly, 16 out of the 23 PKs, for which cleavage sites were characterized, have cleavage sites within 60 residues of their N- or C-termini. We investigated whether these sites were also cleaved *in vivo* when apoptosis was induced by TNFα. For these experiments, CaMKK1, eEF2K, MNK2, AMPKa1, and TRIB3, which were cleaved *in vitro* at D32, D14, D32/D58, D520 (30 residues away from the C-terminus), and D338 (20 residues away from the C-terminus), respectively, were used (Figure 5b and Table 1). Their genes (wild type, WT) were each reconstructed with a V5 tag added at the end opposite the cleavage site. The genes for their D→A mutants (DA), and for the sequences of their longer CASP3-cleaved fragments (C3M), were also constructed and all were expressed in control and in apoptotic cells (Figure 5c). Cleavage of the WT PKs produced long fragments corresponding to C3M in apoptotic cells, whereas z-VAD-FMK blocked cleavage. These cleavages near the N- and

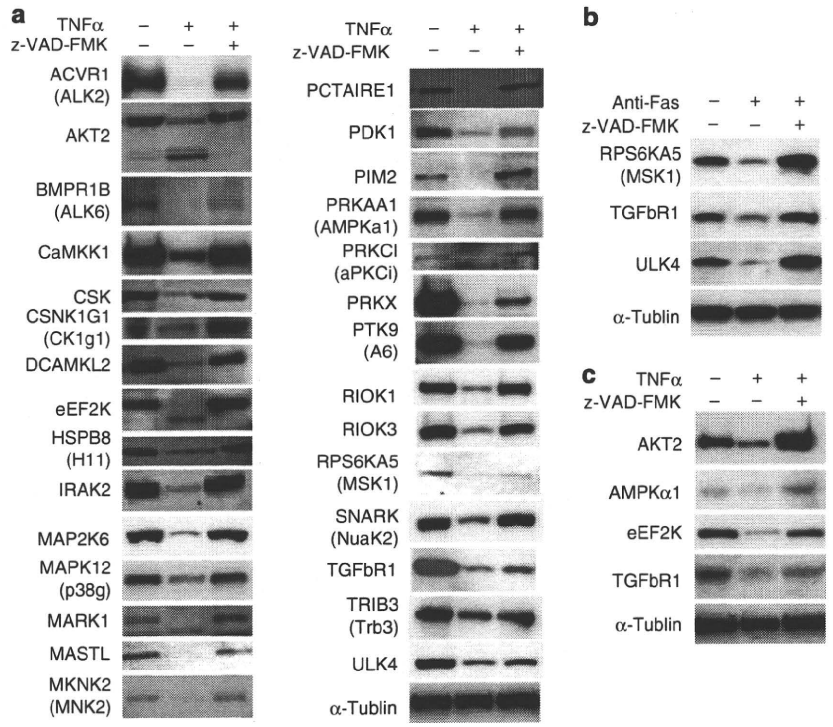

Figure 4 *In vivo* caspase cleavage of the newly identified PK substrates and of endogenous PK substrates. (**a**) *In vivo* cleavage of the $(His)_6$-PK-Flag constructs expressed in apoptotic HeLa cells. The cells were treated with DMSO (control) or with TNFα and cycloheximide (TNFα) in the presence and absence of z-VAD-FMK (a CASP3 inhibitor) for 6 h and then lysed. The cell extracts were immunoblotted and the PK constructs were detected with anti-Flag antibodies, except for HSPB8 and MAP2K6. Anti-His tag antibody was used for the two PKs. (**b**) The cells were transfected with a plasmid of $(His)_6$-PK-Flag constructs, and treated with DMSO (control), or with anti-Fas antibody (anti-Fas) in the presence and absence of z-VAD-FMK for 6 h and then lysed. Immunoblotting was carried out as (**a**). (**c**) HeLa cells were treated as in (**a**), but were not transfected with a *$(His)_6$-PK-Flag* gene. Each endogenous PK was detected using an antibody specific for it. α-Tubulin was used as an internal marker

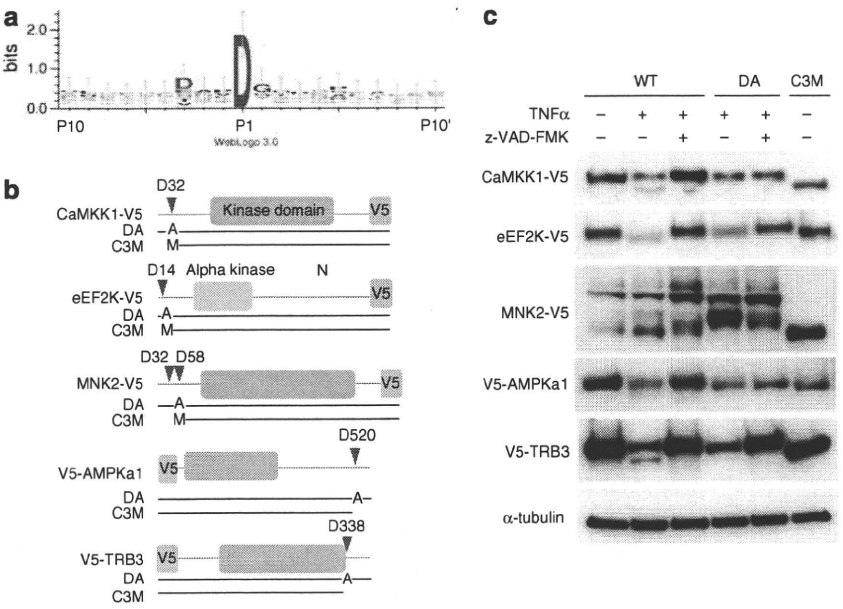

Figure 5 The cleavage site logo and *in vivo* cleavage of five PKs that are cleaved by CASP3 near their N- or C-termini. (**a**) The 20 residues surrounding the D of the hydrolytic bond in 28 PKs were analyzed using WebLogo, version 3.0.[36] (**b**) Cartoons of five PK sequences that have cleavage sites near their N- or C-termini. The corresponding PKs were used for the experiment shown in (**c**). The positions of the alanines in the D → A mutants (DA) are shown, as are the long fragments (C3M) produced by CASP3 cleavage. V5 tags were fused at the ends farther away from the cleavage sites. The first M in C3M of CaMKK1, eEF2K, and MNK2 indicates a methionine as a start amino acid. (**c**) Immunoblots of PK-V5s and V5-PKs that had been expressed in apoptotic HeLa cells. The cells were treated with DMSO (control) or with TNFα and cycloheximide in the presence or absence of z-VAD-FMK for 6 h and then lysed. The proteins were blotted and then detected with anti-V5 antibodies. WT indicates a wild-type protein